iScience

CellPress

Article

Histone Deacetylase-Mediated Müller Glia Reprogramming through Her4.1-Lin28a Axis Is Essential for Retina Regeneration in Zebrafish

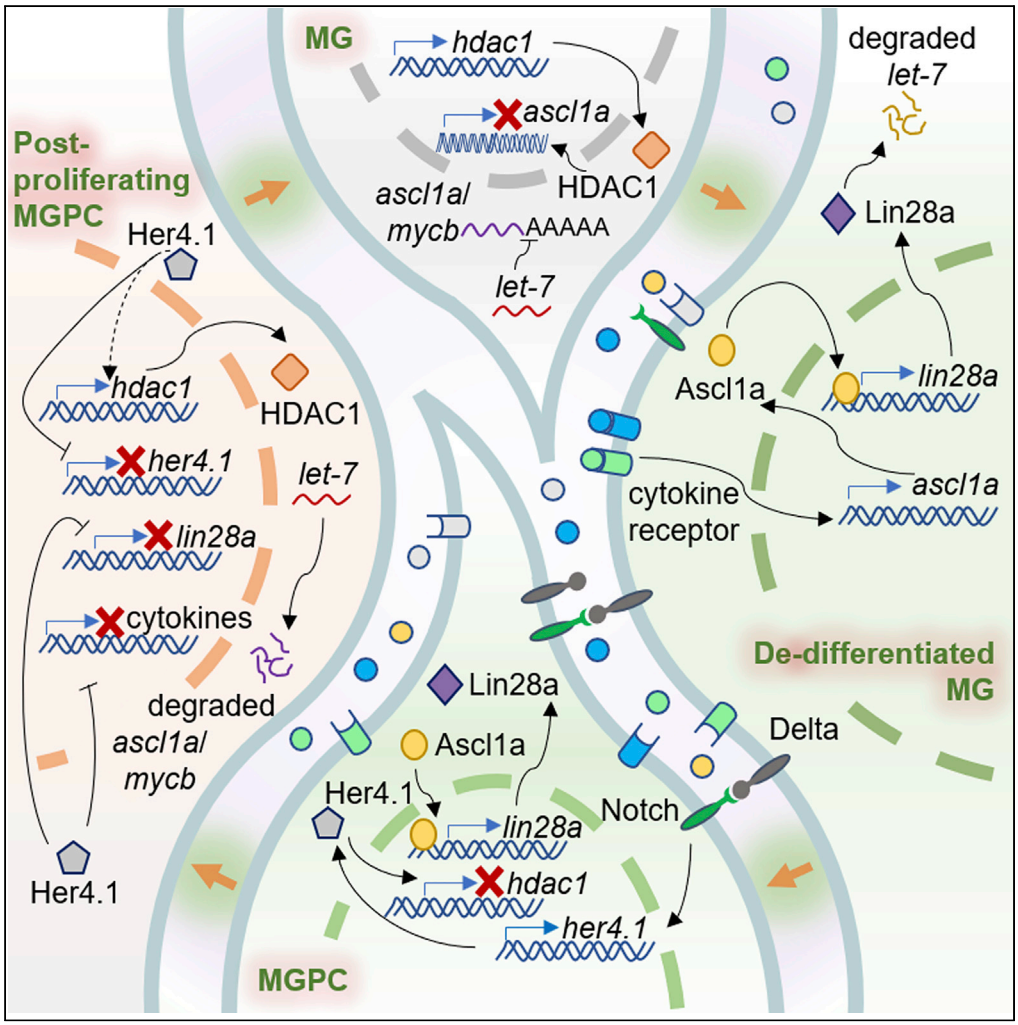

Soumitra Mitra, Poonam Sharma, Simran Kaur, ..., Akshai J. Kurup, Mansi Chaudhary, Rajesh Ramachandran

rajeshra@iisermohali.ac.in

HIGHLIGHTS

Hdac1, along with other Hdacs, is a key regulator of retina regeneration in zebrafish

Hdacs regulate MGPCs' formation through Her4.1/Lin28a/*let-7* miRNA axis

Hdacs' inhibition reversibly blocks MGPCs' proliferation and retina regeneration

Hdacs/Her4.1 interplay regulates essential cytokines during retina regeneration

Mitra et al., iScience 7, 68–84
September 28, 2018
https://doi.org/10.1016/j.isci.2018.08.008

iScience

CellPress

Article

Histone Deacetylase-Mediated Müller Glia Reprogramming through Her4.1-Lin28a Axis Is Essential for Retina Regeneration in Zebrafish

Soumitra Mitra,[1] Poonam Sharma,[1,2] Simran Kaur,[1,2] Mohammad Anwar Khursheed,[1] Shivangi Gupta,[1] Riya Ahuja,[1] Akshai J. Kurup,[1] Mansi Chaudhary,[1] and Rajesh Ramachandran[1,3,*]

SUMMARY

Histone deacetylases (Hdacs) play significant roles in cellular homeostasis and tissue differentiation. Hdacs are well characterized in various systems for their physiological and epigenetic relevance. However, their significance during retina regeneration remains unclear. Here we show that inhibition of Hdac1 causes a decline in regenerative ability, and injury-dependent regulation of *hdacs* is essential for regulating regeneration-associated genes like *ascl1a, lin28a,* and repressors like *her4.1* at the injury site. We show selective seclusion of Hdac1 from the proliferating Müller glia-derived progenitor cells (MGPCs) and its upregulation in the neighboring cells. Hdacs negatively regulate *her4.1*, which also represses *lin28a* and essential cytokines to control MGPCs proliferation. Interestingly, Hdacs' inhibition reversibly blocks regeneration through the repression of critical cytokines and other regeneration-specific genes, which is also revealed by whole-retina RNA sequence analysis. Our study shows mechanistic understanding of the Hdac pathway during zebrafish retina regeneration.

INTRODUCTION

Unlike mammals, vertebrates of piscine and amphibian groups possess very remarkable regenerative potential in almost all tissue types and organs and thus have been studied extensively for a greater understanding of the molecular mechanisms underlying tissue regeneration (Ail and Perron, 2017; Gemberling et al., 2013; Goldman, 2014; Kyritsis et al., 2012; Mokalled et al., 2016; Poss et al., 2002; Rabinowitz et al., 2017; Singh et al., 2012; Wan and Goldman, 2016). Zebrafish, a piscine member, is an excellent model to study the molecular mechanisms of regeneration in complex tissues like brain and retina. Retina regeneration in zebrafish depends mostly on the de-differentiation of Müller glia (MG), which then reprogram themselves to produce progenitor cells with stem cell-like properties (MG-derived progenitor cells [MGPCs]). Later, these MGPCs differentiate into various neurons of the retina and the MG itself with the help of different contributing factors (Fausett and Goldman, 2006; Ramachandran et al., 2010b). These include growth factors (Gramage et al., 2015; Russell, 2003; Wan et al., 2012; Zhao et al., 2014), cytokines (Wan et al., 2014; Zhao et al., 2014), gene transcription factors (Nelson et al., 2012; Ramachandran et al., 2010a, 2012b; Thummel et al., 2010; Wan et al., 2014), epigenome modifiers (Powell et al., 2012, 2013), cell-cycle regulators (Luo et al., 2012; Ramachandran et al., 2011, 2012b), and differentiation factors (Munderloh et al., 2009), which get dynamically regulated with precise orchestration among themselves, leading to the restoration of normal vision (Sherpa et al., 2008). Conversely, mammalian retina often undergoes reactive gliosis upon injury, which eventually leads to scar formation (Bringmann et al., 2009). Although good knowledge of the molecular regulatory networks that form the foundation of regeneration cascade exist in zebrafish, several important gene regulatory networks remain enigmatic. One such unknown territory is the involvement of epigenome modifiers like histone deacetylases (Hdacs). Unraveling crucial gene regulatory network underlying retina regeneration, with temporal and spatial precision, would be possible only through an understanding of the epigenome modifiers such as Hdacs and the subsequent genes involved. Finally, we anticipate that the cellular and molecular regulatory mechanisms that bring about regeneration in the zebrafish could pave the way for curing mammalian retinal damage.

Hdacs usually function as catalysts for the deacetylation of acetyl-L-lysine side chains of histone proteins by forming transcriptional co-repressor complexes, which typically enable the alteration of chromatin structure and repress gene transcription. There are 4 major classes of Hdacs with diverse functions including the modifications of non-histone targets in normal cell biology (Gregoretti et al., 2004). Furthermore,

[1]Indian Institute of Science Education and Research, Mohali, Knowledge City, Room 3F10, Academic Block-1, Sector 81, SAS Nagar, Manauli PO, Mohali, Punjab 140306, India

[2]These authors contributed equally

[3]Lead Contact

*Correspondence: rajeshra@iisermohali.ac.in

https://doi.org/10.1016/j.isci.2018.08.008

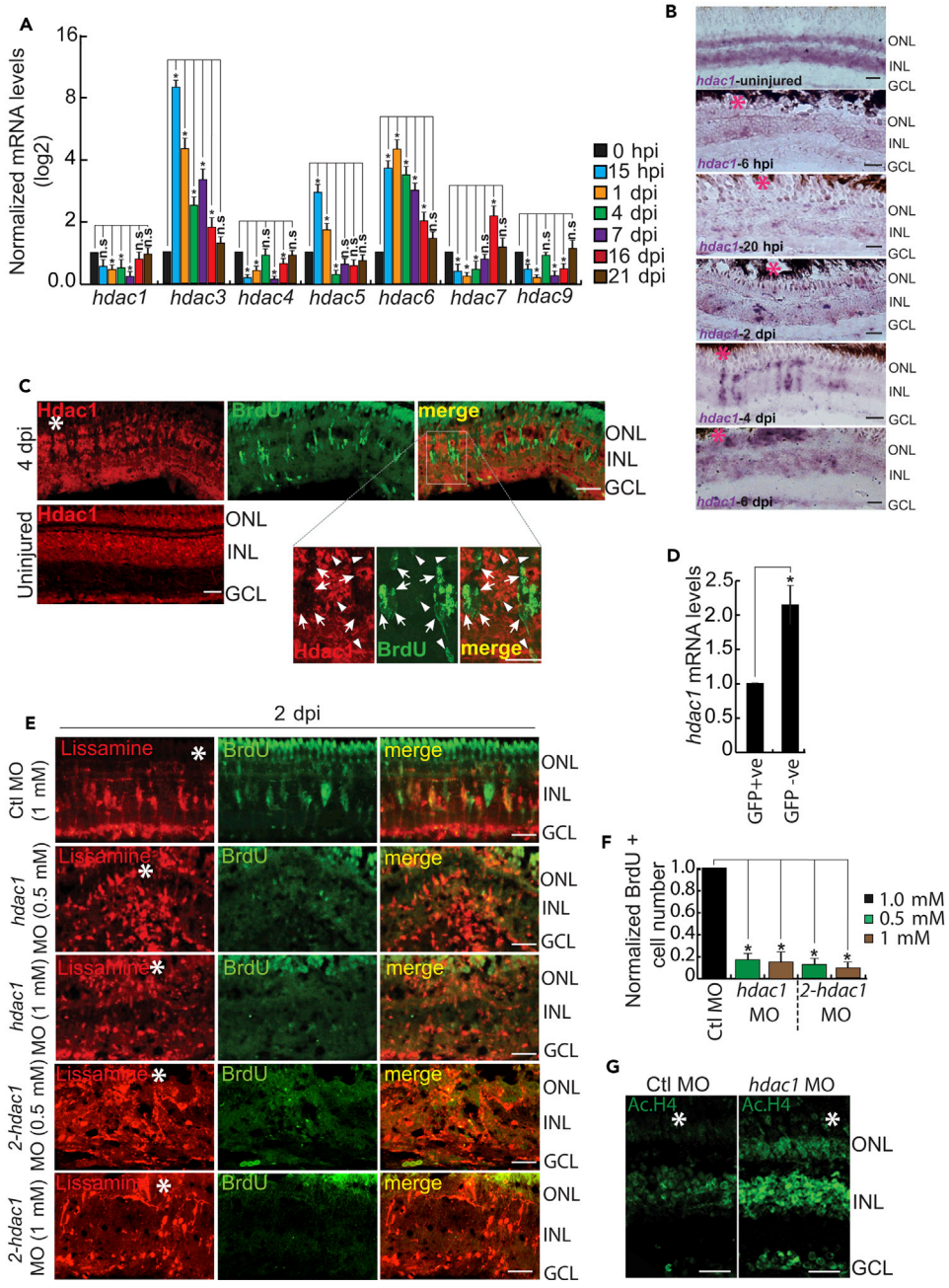

Figure 1. Hdacs' Inhibition Suppresses the Formation of MGPCs

(A) qPCR assay shows injury-dependent regulation of *hdacs*. *p < 0.04, n.s, not significant.

(B) ISH microscopy of *hdac1* expression in uninjured state and at various time points after retinal injury.

(C) Immunofluorescence (IF) microscopy shows that Hdac1 expression is mostly absent from $BrdU^+$ cells at the site of injury, in the retina at 4 dpi. Arrowheads indicate co-labeled $Hdac1^+$ and $BrdU^+$ cells, arrows mark $Hdac1^-$ but $BrdU^+$ cells.

(D) qPCR assay of *hdac1* from GFP-positive and GFP-negative sorted cells from *1016tuba1a*: GFP transgenic retina at 4 dpi. *p<0.002.

(E and F) MO-based *hdac1* knockdown using two different MOs separately decreases $BrdU^+$ cells, relative to the control MO (E), which accounts for 80% reduction in cell number (F) in 2 dpi retina; ANOVA test, *p < 0.001. MOs were delivered at the time of injury, electroporated immediately after injury, and harvested at 2 dpi.

(G) *hdac1* inhibition using antisense MO (0.5 mM) causes upregulation of acetylated histone 4 compared with control (0.5 mM), revealed by IF microscopy in 4 dpi retina.

Figure 1. *Continued*

N = 6 biological replicates in all experiments unless specified. Scale bars, 10 μm in (B, C, E, and G). Error bars are SD. ONL, outer nuclear layer; INL, inner nuclear layer; GCL, ganglion cell layer. The asterisk marks the injury site in (B, C, E, and G). See also Figures S1 and S2.

HDAC inhibitors are of immense interest to the research and medical communities, which focus on tackling their anti-cancer properties to develop them as potential tools for cancer treatment (Lombardi et al., 2011; Witt et al., 2009). Hdac1 knockout is embryonically lethal in mice and is known to cause cell proliferation defects through the upregulation of cyclin-dependent kinase inhibitors like p21 and p27 (Lagger et al., 2002; Montgomery et al., 2007; Witt et al., 2009). The decline in Hdac1 is also associated with a decrease in overall Hdac activity exhibited by other Hdacs, which is usually not complemented by overexpression of Hdac2 or Hdac3 (Lagger et al., 2002; Montgomery et al., 2007; Witt et al., 2009). These attributes along with its near-ubiquitous expression make Hdac1 unique, which demands further exploration in regeneration biology of the retina. Hdac1 being part of multi-protein nuclear complexes that are important for causing transcriptional repression and epigenetic landscaping to inhibit the expression of neuronal-specific genes in rest of the tissues (Huang et al., 1999) made us explore the global gene regulations that occur in MGPCs mediated through Hdacs with a particular focus on Hdac1. Furthermore, MG reprogramming leading to induction of MGPCs, with little neuronal characteristics, during retina regeneration is associated with essential expression of pluripotency-inducing factors (Gorsuch et al., 2017; Ramachandran et al., 2010a; Reyes-Aguirre and Lamas, 2016), which could also be targets of epigenome modifiers like Hdacs.

Here we unravel the unique roles played by Hdacs in regulating the expression of various regeneration-associated essential genes like *mycb*, *ascl1a*, *lin28a*, *insm1a*, and *her4.1* during MG reprogramming and induction of MGPCs. We also show the global changes in gene expression with compromised Hdac function during regeneration, through a whole retina RNA sequencing (RNA-seq) analysis. Furthermore, we unravel a few novel gene regulatory networks that connect Hdacs with Delta-Notch signaling, *lin28a*, and a few essential cytokines. We also show the importance of Hdacs in regulating *her4.1* to restrict *lin28a* expression, which is a necessity for the translation of various genes like *ascl1a*, and *mycb* through the suppression of *let-7* microRNA. Our study, therefore, unravels the hitherto unknown facts about Hdacs to bring about the induction of MGPCs for successful retina regeneration.

RESULTS

Hdacs Are Necessary for MGPCs' Induction after Retinal Injury

There are different methods to study regeneration, of which needle poke is quicker, more natural, and less traumatic to the fishes. In this method, we injure the retina of fish using a 30G needle after administering deep anesthesia and harvest the eye at various time points. Analysis of *hdac*s gene expression following retinal injury revealed that *hdac3*, *hdac5*, and *hdac6* get rapidly induced and *hdac1*, *hdac4*, *hdac7*, and *hdac9* get downregulated (Figure 1A). The mRNA *in situ* hybridization (ISH) analysis revealed a panretinal expression of *hdac1* in the uninjured retina, which declines drastically after an injury. Although the mRNA of *hdac1* reappeared near the injury spot at 4 days post-injury (dpi), interestingly, it showed exclusion from the majority of bromodeoxyuridine^{+} (BrdU^{+}) cells and co-localized with only a fraction of progenitors (Figures 1B, S1A, and S1B). We saw a similar pattern of expression for *hdac3*, *hdac4*, *hdac5*, *hdac6*, and *hdac9* (Figures S1C–S1L). The cell count data of *hdac1*-expressing cells showed an increased co-localization with proliferating cell nuclear antigen (PCNA) compared with the ones having just BrdU (Figure S1B). PCNA, a molecule with a longer half-life and an ability to stay detectable even after cell-cycle exit (Bologna-Molina et al., 2013; Kimmel and Meyer, 2010; Mandyam et al., 2007), could efficiently be used as an indicator of post-proliferative status as well. From our results, the increased co-localization of *hdac1* with PCNA compared with BrdU pulse-labeled cells suggests that *hdac1* gets upregulated in post-proliferative MGPCs. Interestingly, immunofluorescence showed a drastic decline in Hdac1 protein expression in MGPCs at 4 dpi (Figure 1C), but we found a higher percentage co-labeling with BrdU, at 2 and 6 dpi (Figure S2A). However, no significant temporal variation was seen in Hdac1 protein levels at different time points post injury in the whole retinal extract (Figure S2B).

We further conducted experiments using transgenic fish that marks proliferating MGPCs in the retina. For this, a *1016tuba1a*: GFP transgenic zebrafish, which is well characterized to mark proliferating MG-derived progenitors after an injury (Fausett and Goldman, 2006), was used. Furthermore, the *1016tuba1a*: *Cre*-ERT2/β-actin-LCLG double transgenic fish was used in previous studies to identify the lineage of the

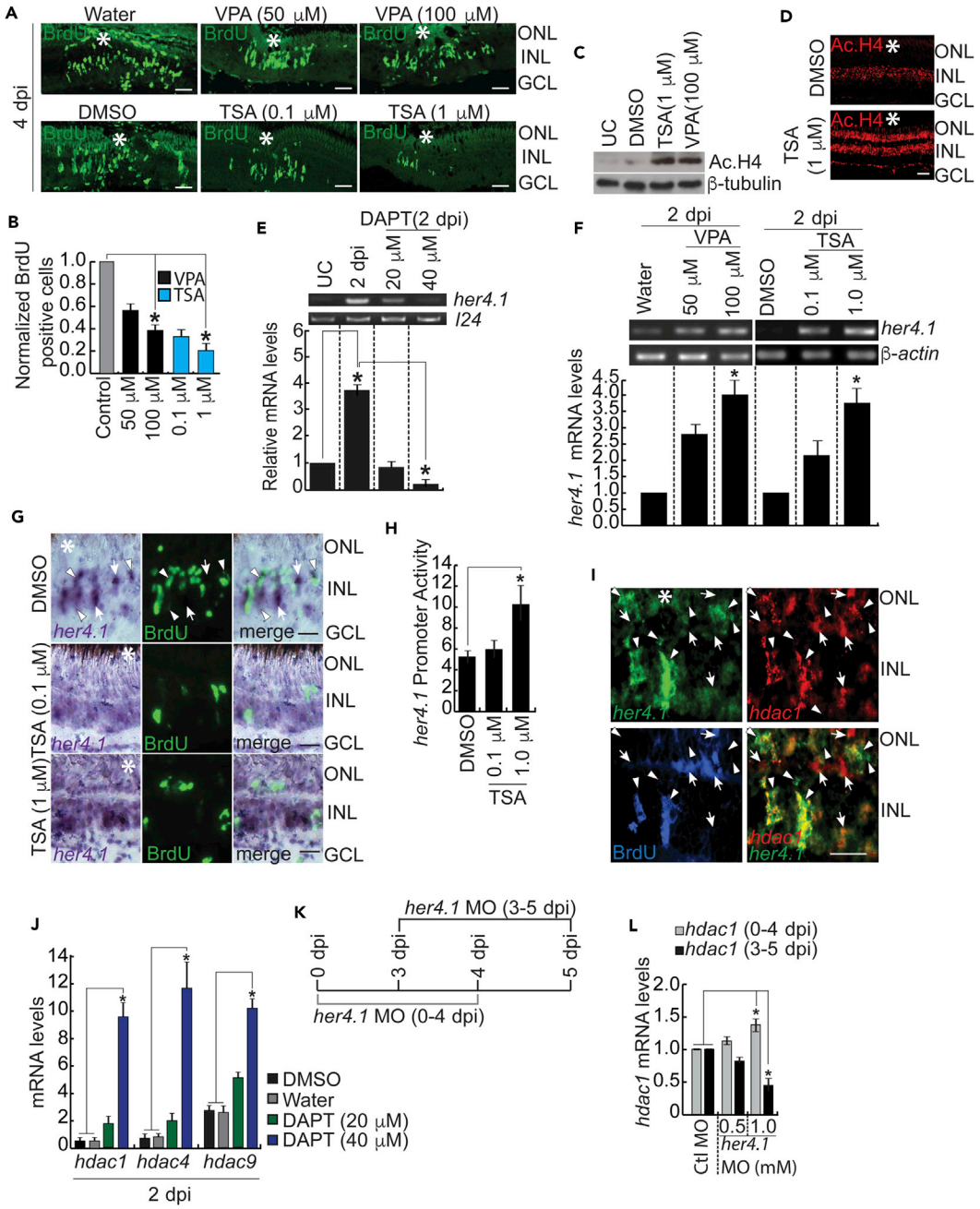

Figure 2. Hdacs and Her4.1 Mutually Inhibit Each Other during MGPCs-Mediated Retina Regeneration

(A and B) Immunofluorescence (IF) microscopy on retinal sections shows a reduction in the number of proliferating MGPCs following Hdacs' inhibition by VPA and TSA at 4 dpi (A), which is quantified in (B); ANOVA test, *p < 0.0001 in (B).

(C and D) Western blot analysis revealed upregulated acetylated histone 4 with Hdacs inhibition at 2 dpi retina (C) and IF microscopy at 4 dpi (D), compared with uninjured and DMSO-treated control retina.

(E) RT-PCR (upper) and qPCR (lower) of *her4.1* mRNA in DAPT-treated retina, compared with uninjured (UC) and 2 dpi retina. *p < 0.001.

(F and G) RT-PCR (upper) and qPCR (lower) (F) and ISH and IF microscopies in 4 dpi retina (G) show that Hdac blocker VPA/TSA increases *her4.1* induction compared with respective controls. Arrowheads indicate co-labeled *her4.1*$^{+}$ and BrdU^{+} cells, arrows mark *her4.1*$^{+}$ but BrdU^{-} cells in (G). *p < 0.0001 in (F).

(H) Single-cell-stage embryos were injected with *her4.1:luciferase* vector along with Renilla luciferase mRNA for normalization, which were then treated with TSA for 24 hr before lysing for quantification of *her4.1* promoter activity by dual luciferase assay. *p < 0.003.

(I) Fluorescence *in situ* hybridization and IF microscopy show co-localization of *her4.1* and *hdac1* with BrdU^{+} MGPCs in 4 dpi retina. Arrowheads indicate *her4.1*$^{+}$ and *hdac1*$^{-}$ cells, arrows mark *her4.1*$^{-}$ but *hdac1*$^{+}$ cells.

(J) qPCR of *hdac1*, *hdac4*, and *hdac9* mRNAs with blockade of Notch signaling by DAPT treatment, in 2 dpi retina; *p < 0.002.

Figure 2. *Continued*

(K) Schematic experimental timelines for *her4.1* MO electroporation in the retina.

(L) qPCR of *hdac1* in *the her4.1* knockdown retina as per the experimental timeline in (K); *p < 0.03.

N = 4 biological replicates in all experiments. Scale bars, 10 μm in (A, D, and G) and 20 μm in (I). The asterisk marks the injury site in (A, D, G, and I). ONL, outer nuclear layer; INL, inner nuclear layer; GCL, ganglion cell layer. See also Figures S2, S4, and S6.

MG-derived progenitors in regenerating zebrafish retina (Ramachandran et al., 2010b, 2012a). Using this *1016tuba1a*: GFP transgenic zebrafish, we sorted the GFP-positive and GFP-negative cell populations from the injured retina to explore the levels of *hdac1* mRNA. Interestingly, we found significant downregulation of *hdac1* mRNA in the GFP-positive population, compared with the rest of the cells (Figure 1D), suggesting that GFP-positive MGPCs need to have a declined *hdac1* expression for a successful regenerative response of the retina. These observations indicate that Hdac1-mediated gene regulation is prevalent both in MGs that are yet to dedifferentiate and enter the cell cycle and in post-proliferative MGPCs.

To investigate the role of Hdac1 during regeneration, *hdac1*-targeting morpholino (MO), which blocked its protein expression, was used (Figures S2C and S2D). The *hdac1*-targeting MOs were delivered separately and electroporated at the time of injury and harvested at 2 dpi, which resulted in 80% decline in the number of proliferating cells (Figures 1E, 1F, S2E, and S2F). Transfection of *hdac1* and *gfp* reporter mRNA along with the respective MO that does not bind onto the delivered mRNA could rescue the reduction in cell proliferation in the retina at 2 dpi (Figures S3A and S3B). We also found an enhanced proliferation with *gfp-hdac1* fusion mRNA transfection in these rescue experiments (Figures S3A and S3B).

We then decided to explore the specific effect of *hdac1* knockdown on cell proliferation in the early and late proliferative phases of regeneration. For this, we performed late *hdac1* knockdown experiments in which the retina is allowed to regenerate until 2 or 4 dpi and then electroporated with *hdac1* MO and harvested at 4 or 6 dpi, respectively (Figures S3D–S3I). Although we delivered the MO during injury, it remains dormant in the vitreous until electroporated to get entry into the retina enabling *hdac1* knockdown. In both these sets, we found a decline in the MGPCs marked by PCNA compared with the control MO group, as observed in the 0–2 dpi *hdac1*-knockdown groups. MO-mediated *hdac1* repression also caused an upregulation of acetylated histone 4 (Ac.H4) in the retina, which demonstrated the efficacy of Hdac inhibition (Figure 1G). These findings suggest the existence of *hdac1*-mediated gene regulation in normal reprogramming and perpetuation of retina regeneration.

Furthermore, we explored the effect of the global decline in Hdac activity through well-characterized pharmacological inhibitors of Hdacs, valproic acid (VPA) and trichostatin A (TSA) separately (Bolden et al., 2006; Xu et al., 2007). We found that proliferation decreased up to 80% in VPA or TSA, and we reasoned that Hdacs could be associated with MGPCs induction in the retina, at 4 dpi (Figures 2A and 2B). The reduction in the number of MGPCs seen with VPA or TSA treatment was not because of apoptosis (Figures S4A–S4C) or DMSO in the drug as the solvent (Figures S4D and S4E). Furthermore, we observed increased levels of Ac.H4 by VPA and TSA treatment in the post-injured retina (Figures 2C, 2D, and S4F). These results suggest the existence of Hdac-mediated gene regulatory pathway, which is necessary for the induction of retinal MGPCs during regeneration.

We also performed a whole-retina RNAseq analysis, to explore the changes in global gene expression that occur with the compromised activity of Hdacs. For this, we used total retina isolated from zebrafish of, uninjured (UC), 12 hours post injury (hpi), 4 dpi, and VPA-treated 4 dpi experimental groups. The VPA-mediated Hdacs' inhibition revealed several transcription factors that are up- or downregulated when compared with 12 hpi and 4 dpi (Table S2; Figures S4G and S4H) (GEO accession: GSE98094), including several regeneration-associated genes, namely, *ascl1a*, *mycb*, *lin28a*, *foxn4,* and *insm1a* (Goldman, 2014; Kaur et al., 2018; Ramachandran et al., 2010a, 2011, 2012b). We further evaluated the molecular mechanisms of regulation of a few of these genes with regard to normal and deregulated activity of Hdacs.

Hdacs-Her4.1 Interplay Governs MGPCs Proliferation

Next, we explored the possible reasons for the MGPCs induction to be diminished upon Hdacs' suppression. One such candidate gene was a Delta-Notch effector gene *her4.1*. We chose *her4.1* mainly because of its negative regulation on retina regeneration. Forced expression of *notch intracellular domain* (*nicd*), which upregulates *her4.1*, is known to repress MGPCs induction completely, whereas pharmacological

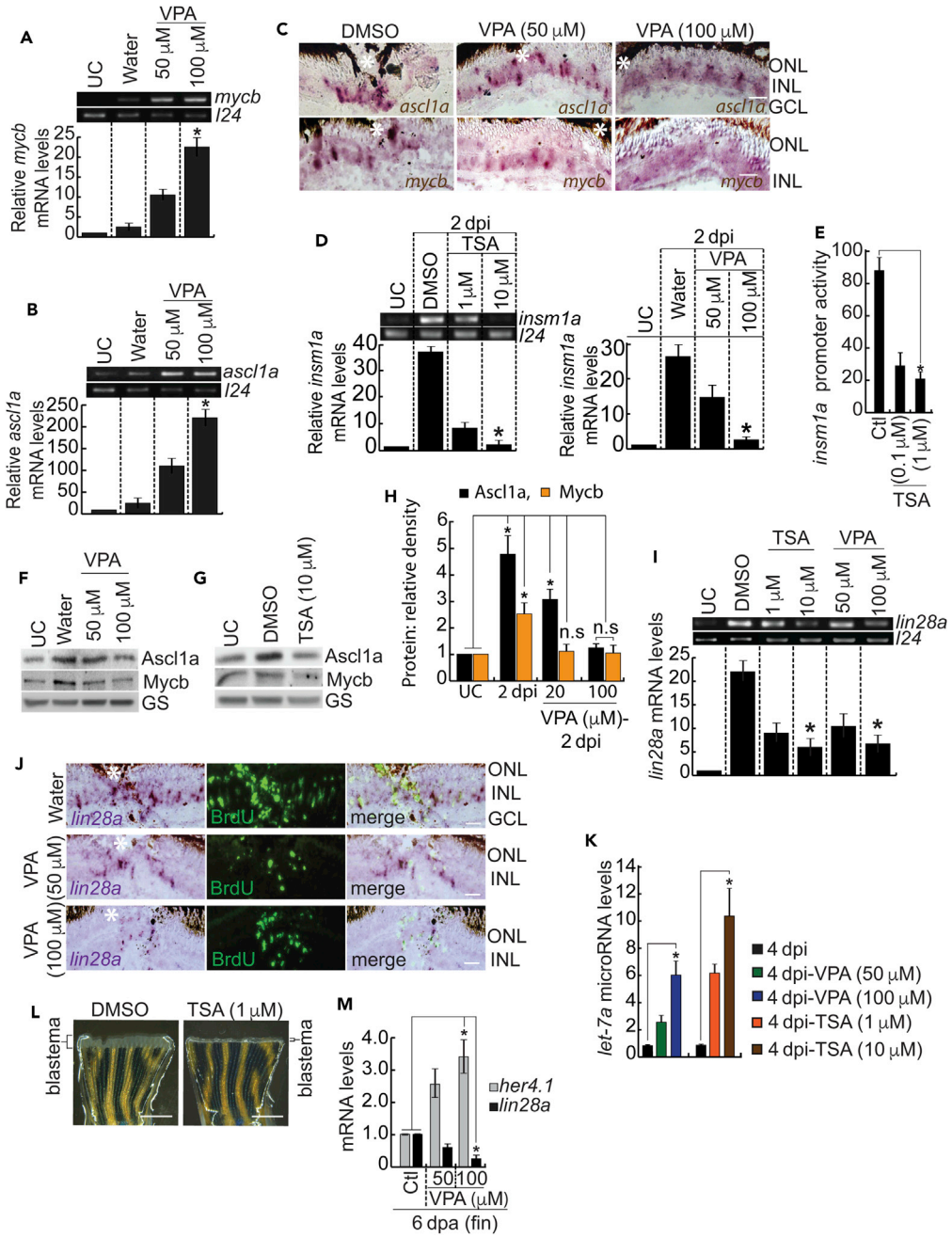

Figure 3. Hdacs' Repression Causes Upregulation of *ascl1a* and *mycb*, and Repression of *insm1a* and *lin28a*

(A and B) RT-PCR (upper) and qPCR (lower) show upregulation of *mycb* (A) and *ascl1a* (B) with VPA-mediated Hdacs' repression, relative to the control in 2 dpi retina; *p < 0.0001.

(C) ISH microscopy reveals that *ascl1a* and *mycb* mRNAs show an expanded zone of expression at 4 dpi, with VPA.

(D) RT-PCR (upper) and qPCR (lower) show downregulation of *insm1a* in Hdacs' blockers TSA (left) and VPA (right) by qPCR, relative to the control in 2 dpi retina. *p < 0.003.

(E) Hdacs' repression using TSA inhibits luciferase activity in 24 hours post fertilization embryos injected with *insm1a:gfp-luciferase* vector; *p < 0.0002.

(F and G) Western blot analysis reveals a decline in Ascl1a and Myc protein levels in 2 dpi retina treated with VPA (F) and TSA (G), compared with control. GS, glutamine synthetase; it is the loading control.

(H) Densitometry analysis of western blots from (F), done in triplicates. *p < 0.003, n.s, not significant.

Figure 3. *Continued*

(I and J) RT-PCR (upper) and qPCR (lower) show a decline in *lin28a* expression at 2 dpi retina (I), confirmed by ISH microscopy (J), with VPA-mediated Hdacs' repression, compared with the control in 4 dpi retina; ANOVA test, *p < 0.0002 in (I). N = 3 biological replicates.

(K) qPCR analysis of the *let-7a* microRNA shows an upregulation with VPA/TSA treatment in 4 dpi retina. *p < 0.001.

(L) TSA-treated 3 dpa fin shows a reduction in blastema compared with DMSO control.

(M) qPCR analysis of the VPA-treated fin blastema shows an increase in *her4.1* and decrease in *lin28a* mRNA levels at 6 dpa compared with control. *p < 0.002.

Scale bars, 10 μm in (C and J) and 500 μm in (L). The asterisk marks the injury site in (C and J). ONL, outer nuclear layer; INL, inner nuclear layer; GCL, ganglion cell layer. See also Figures S3–S6.

inhibition of γ-secretase through the drug DAPT (*N*-[*N*-(3,5-difluorophenylacetyl)-L-alanyl]-*S*-phenylglycine-*t*-butyl ester), which decreases *her4.1* levels, caused an enhancement of the zone of proliferation in injured retina (Conner et al., 2014; Wan et al., 2012) (Figures 2E and S4I).

Interestingly, with Hdacs' inhibition, we found a dose-dependent increase in *her4.1* expression in RT-PCR, qPCR, and mRNA ISH in both VPA- and TSA-treated post-injured retina (Figures 2F and 2G). The blockade of Hdacs reflects a decline in BrdU pulse-labeled MGPCs with a concomitant increase in *her4.1* levels in the retina (Figure 2G). Furthermore, the injection of *her4.1:gfp-luciferase* reporter in zebrafish embryos exposed to TSA confirmed the *her4.1* gene upregulation by the inhibition of Hdacs (Figure 2H). Moreover, the VPA/TSA-treatment-associated increase in *her4.1* expression could be caused by the upregulation of *delta* and *notch* genes (Figures S5A and S5B), as discussed earlier (Figures 2F–2H).

We further explored if the increased *her4.1* levels seen in TSA-treated retina influenced the *hdac1* mRNA levels in the post-injured retina. We found an anticipated decline in *hdac1* mRNA levels revealed by mRNA ISH in TSA-treated 4 dpi retina (Figure S5C). These results suggest the existence of Her4.1-mediated repression of *hdac1* expression. In another scenario, the Hdac1 protein levels also declined in the uninjured retina with VPA treatment in a dose-dependent manner (Figure S5D).

Further analysis by double mRNA ISH of *hdac1* and *her4.1* showed their co-expression in a limited number of cells at 4 dpi (Figure 2I). We also found several *hdac1*-positive cells that are *her4.1* negative, and *vice versa*. Furthermore, the DAPT-mediated inhibition of Delta-Notch signaling, which brings down *her4.1* levels (Conner et al., 2014; Wan et al., 2012) (Figures 2E and S4I), caused an enhancement of *hdac1*, *hdac4,* and *hdac9* expression at 2 dpi (Figure 2J). It is interesting to note that *hdac1*, *hdac4*, and *hdac9* showed a similar temporal expression pattern post-retinal injury (Figure 1A). This observation supports the possibility that these three genes are regulated similarly. Furthermore, to confirm the influence of Her4.1 on *hdac1* expression, we employed MO-based gene knockdown approach. We analyzed the efficacy of *her4.1*-targeting MO in zebrafish embryos by co-injection with a construct harboring MO-binding sequence appended to GFP along with *her4.1* or control MO (Figure S2D). Similarly, we saw upregulation of *hdac1* expression with the *her4.1* knockdown from 0 to 4 dpi (Figures 2K and 2L). Notably, the *hdac1* expression from its earlier panretinal nature, immediately after the injury, stayed restricted to the neighboring cells of MGPCs. This type of *hdac1* expression could be a post-proliferative phenomenon seen from its increased co-labeling with PCNA (Figure S1B). Her4.1-mediated gene repression may be a potential cause for this. This speculation is also because of the increased *her4.1* expression in neighboring cells of actively proliferating MGPCs in the injured retina at 4 dpi (Figures S5E and S5F). At later stages of regeneration, this type of Her4.1 expression probably necessitates the stringent regulation of Hdac1 expression in the neighboring cells of actively proliferating MGPCs. It is mainly evident from the decline in the *hdac1* levels in a *her4.1*-repressed scenario from 3 to 5 dpi (Figures 2K and 2L). It is also important to note that if *her4.1* is inhibited immediately after the retinal injury, we found an increase in *hdac1* expression (Figure 2L). These findings suggest that Her4.1 has a role in *hdac1* repression at early stages that is just opposite at later stages of regeneration. These results presumably indicate a mutual but differential regulation between Her4.1 and Hdac1 during various phases of regeneration.

lin28a Expression Mediated through Hdacs Is Necessary during Retina Regeneration

Furthermore, we probed for the expression pattern of regeneration-associated genes like *mycb*, *ascl1a*, and *insm1a* in VPA/TSA-treated retina. Interestingly, we found an increase in the expression of genes *mycb* and *ascl1a*, and a sharp decline in *insm1a* levels, in the VPA-treated injured retina (Figures 3A–3D) and luciferase assay done in zebrafish embryos (Figure 3E). The decrease in *insm1a*, a transcriptional

repressor (Ramachandran et al., 2012b), also may contribute to enhanced *mycb* and *ascl1a* levels. The *ascl1a* and *mycb* were also regulated similarly with the *hdac1* knockdown in the retina (Figures S6A–S6C). Surprisingly, the increased mRNA levels of *ascl1a* and *mycb* seen in Hdac-inhibited retina did not show a corresponding increase in their protein levels, which instead decreased (Figures 3F–3H). We speculated that lack of Lin28a-mediated suppression of *let-7* microRNA could be the possible reason for reduced protein translation of Ascl1a and Myc from their mRNAs, as described earlier (Ramachandran et al., 2010a). We found a significant reduction in *lin28a* expression in Hdacs-inhibited retina after injury (Figures 3I, 3J, S6A, S6D, and S6E). Furthermore, the cell proliferation results in rescue experiments (Figure S3A and S3B) may also be because of changes in *lin28a* mRNA levels (Figure S3C). The reduction in *lin28a* levels caused an anticipated increase in the *let-7* microRNA in TSA/VPA-treated retina (Figure 3K). The abundant *let-7* microRNA could block the translation of regeneration-associated mRNA such as *ascl1a* and *mycb*, which justified the reduced protein levels of Ascl1a and Mycb (Figures 3F–3H).

Interestingly, the regenerating caudal fin blastema also showed a decrease in cell mass in response to TSA-mediated Hdac inhibition (Figure 3L). Furthermore, we observed increased levels of Ac.H4 by VPA/TSA treatment in 6 days post amputation (dpa) fin blastema (Figure S6F) as found in the post-injured retina (Figures 2C, 2D, and S4F). Interestingly, Hdac inhibition-mediated decline in fin blastema also showed increased *her4.1* and decreased *lin28a* levels (Figure 3M), similar to that seen in the retina (Figures 2F and 3I). These results suggest the existence of a possibly conserved Hdac-dependent gene regulatory pathway during the regeneration of various tissues.

Inhibition of Hdacs, the facilitators of transcriptional repression, caused a decline in the expression of genes like *lin28a*, which seemed a puzzle. However, our previous results suggested the existence of a potential transcriptional repressor such as Her4.1, which in TSA-treated retina stays upregulated (Figures 2F and 2G). This enhancement of *her4.1* could mediate the decline in the expression of *lin28a*.

Her4.1 Directly Represses the Expression of *lin28a* in Injured Retina

Since we found an upregulation of *her4.1* and downregulation of *lin28a* in Hdacs-inhibited retina, we explored whether Her4.1 had any direct effect on the expression levels of *lin28a*. We first examined the impact of reduced *her4.1*, caused by DAPT treatment, on *lin28a* promoter activity in zebrafish embryos, injected with *lin28a:gfp-luciferase* construct. The luciferase assay showed an increased promoter activity in a dose-dependent manner (Figure 4A), which supported this view. To ascertain further the involvement of Her4.1 in *lin28a* expression, we examined its promoter for potential Her/Hes binding sites (Kageyama et al., 2007) and found two putative binding sites (Figure 4B). At first, we validated if the *her4.1:gfp-luciferase* construct showed upregulation of promoter activity with *nicd* mRNA co-injected in zebrafish embryos. We found an expected upregulation of *her4.1* promoter activity in a dose-dependent manner (Figure 4C). We then co-injected zebrafish embryos with *lin28a:gfp-luciferase* reporter bearing either wild-type or mutated Her/Hes binding sites on *lin28a* promoter separately, along with increasing concentrations of *nicd* mRNA. We found that NICD overexpression caused a dose-dependent downregulation of *lin28a* promoter activity in the wild-type construct, which was absent in the mutant. These results showed that Her/Hes binding onto *lin28a* promoter negatively contributes to its functionality (Figure 4D). Fluorescence ISH analysis revealed that many *her4.1*-expressing cells showed weak *lin28a* levels, and *vice versa* (Figure 4E). This observation also suggested the existence of a Her4.1-mediated *lin28a* repression in retinal MGPCs. Furthermore, the knockdown of *her4.1* during the active proliferative phase of regeneration also confirmed these results. We found that blockade of *her4.1* from 3 to 5dpi caused an increase in *lin28a* levels in the retina (Figures 4F and 4G). Furthermore, the late knockdown of *her4.1* also caused a significant increase in the $BrdU^+$ MGPCs in the retina (Figures 4H–4J), probably because of increased *lin28a* expression as demonstrated before (Elsaeidi et al., 2018; Ramachandran et al., 2010a). These results supported the earlier conjecture that Hdacs upregulated the expression of *lin28a* through downregulation of a repressor like Her4.1.

Hdac Inhibition Reversibly Suppresses MGPCs' Formation and Differentiation

We further investigated whether inhibition of Hdacs had a long-lasting impact on retina regeneration. To address this, we performed two sets of experiments. In the first one, fish were dipped in VPA from the time of injury until 4 dpi, immediately an intraperitoneal injection of BrdU was administered, and the eyes were harvested at 8 dpi (Figure 5A). In the second set, we performed the same experiment, except that the BrdU pulsing was given at 8 dpi and eyes were harvested after 5 hr (Figure 5D). These experiments were intended to demarcate the difference in performance of MGPCs with Hdacs' inhibition and after its withdrawal. In the

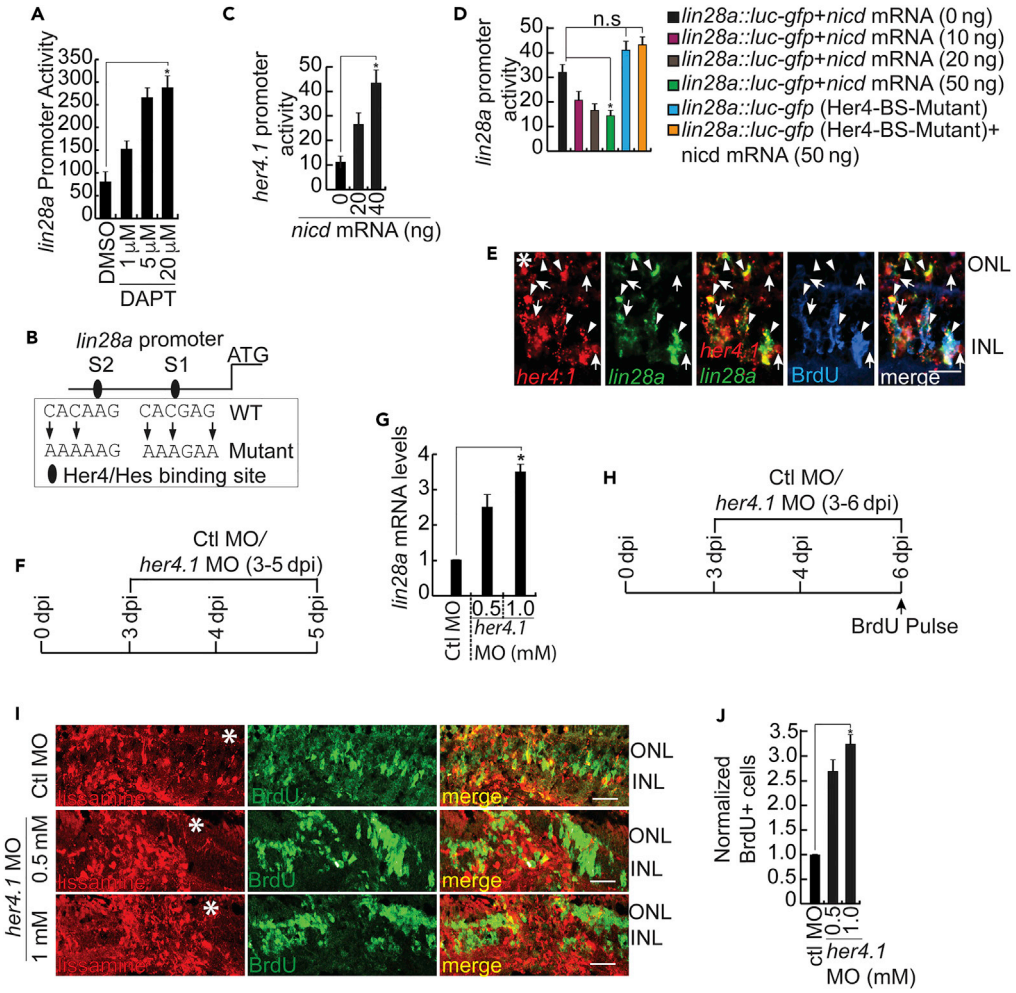

Figure 4. Her4.1 Restricts the Zone of MGPCs by Suppressing *lin28a* Expression

(A) Notch inhibition by DAPT stimulates luciferase activity in 24 hours post fertilization (hpf) embryos injected with *lin28a:gfp-luciferase* vector. *p < 0.0001.

(B) Diagram of *lin28a* promoter with putative Her/Hes binding sites.

(C) NICD overexpression stimulates luciferase activity in 24 hpf embryos injected with *her4.1:gfp-luciferase* vector compared with control. *p < 0.0002.

(D) NICD regulates *lin28a* promoter-driven reporter activity in zebrafish embryos, co-injected with *lin28a:gfp-luciferase* construct and *nicd* mRNA, through the Her/Hes binding sites on the *lin28a* promoter, relative to 0 ng *nicd* mRNA; *p < 0.005; n.s, not significant.

(E) Fluorescence *in situ* hybridization microscopy shows mutual exclusion of *her4.1* and *lin28a*, and IF marks $BrdU^+$ MGPCs in 4 dpi retina. Arrowheads indicate co-labeled $her4.1^+$ and $lin28a^+$ cells, arrows indicate $her4.1^+$ but $lin28a^-$ cells.

(F) Schematic of experimental timelines for *her4.1* MO electroporation.

(G) qPCR of *lin28a* in *her4.1* knockdown retina as per experimental timeline in (F). *p<0.001.

(H–J) Experimental timelines for *her4.1* MO electroporation (H); immunofluorescence microscopy shows increased number of $BrdU^+$ cells in retinal sections electroporated with lissamine-tagged *her4.1* MO as per H (I); quantification of $BrdU^+$ cells seen with late knockdown of *her4.1* in (I) (J); *p < 0.0002 in (J).

N = 3 biological replicates in all experiments. Scale bars, 10 μm in (E and I). The asterisk marks the injury site in (E and I). ONL, outer nuclear layer; INL, inner nuclear layer; GCL, ganglion cell layer. See also Figures S2–S6.

first set, we found a decline in $BrdU^+$ cells at 8 dpi as a result of reduced proliferation at 4 dpi with VPA treatment. Interestingly, we found a significant increase in PCNA-positive cells in 8 dpi as opposed to control (Figures 5B and 5C). In the second set, we found a significant increase in $BrdU^+$ cells, which mostly co-labeled with $PCNA^+$ cells at 8 dpi (Figures 5E and 5F). These observations support the view that in the absence of Hdacs' inhibition the $BrdU^+$ cells seen at 8 dpi are newly formed MGPCs.

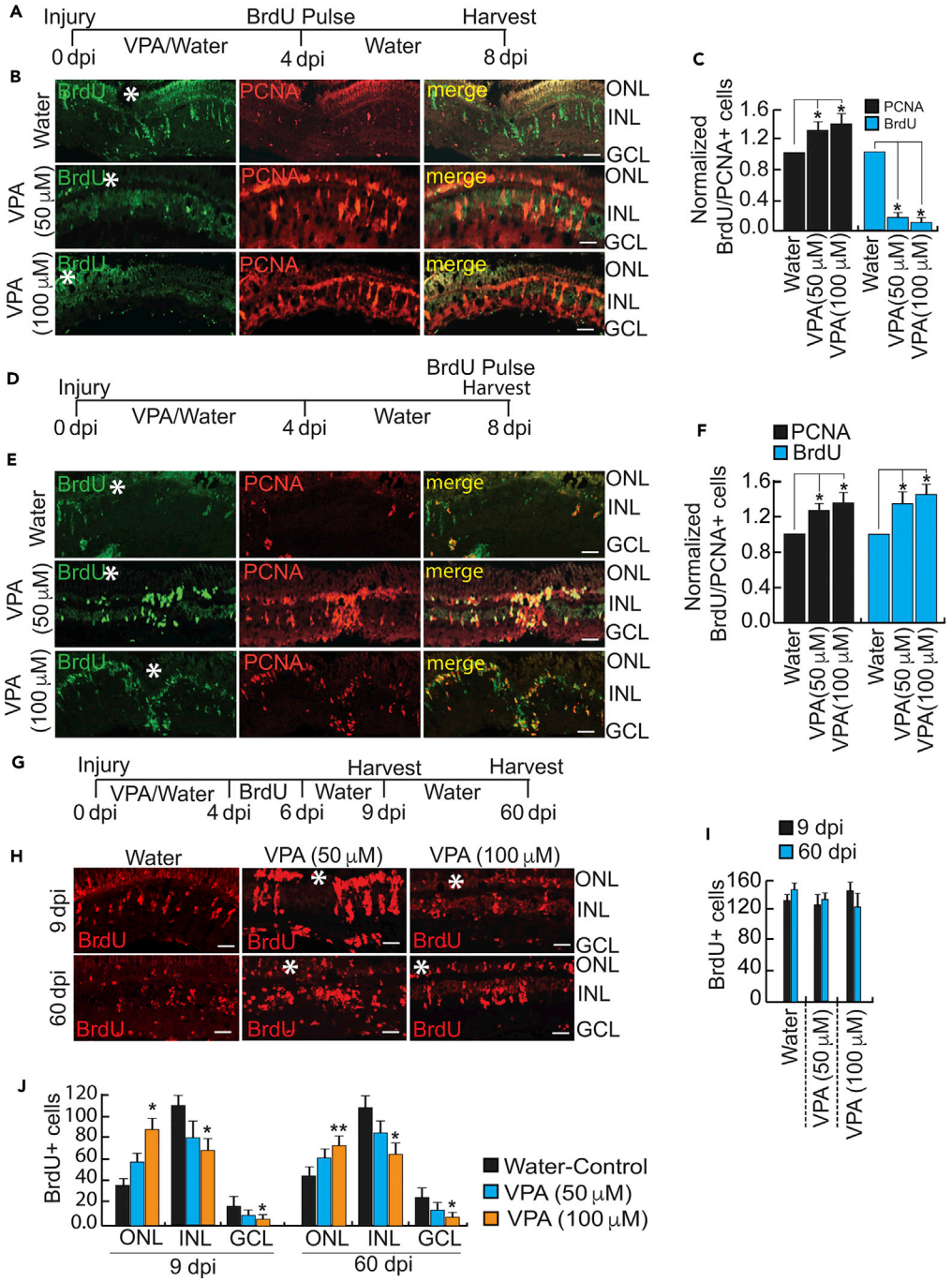

Figure 5. Hdacs' Inhibition Reversibly Suppress MGPCs' Formation and Differentiation

(A–C) An experimental timeline showing VPA treatment from 0 to 4 dpi, BrdU pulse on 4 dpi, and harvest on 8 dpi (A), which shows the re-induction of $PCNA^+$ and minimal $BrdU^+$ proliferating cells revealed by immunofluorescence (IF) microscopy, compared with control (B), quantified in (C); ANOVA test, *$p < 0.01$ in (C).

(D–F) An experimental timeline showing VPA treatment from 0 to 4 dpi and a BrdU pulse done on 8 dpi (D) shows co-labeling of $BrdU^+$ and $PCNA^+$ cells in the re-induced MGPCs in VPA-treated retina and minimal proliferating cells in control, which is revealed by IF microscopy (E), which is quantified in (F); ANOVA test, *$p < 0.01$ in (F).

(G–J) The temporal evaluation of re-induced MGPCs, which are labeled with BrdU in an experiment timeline (G), which reveals that the regeneration occurs similar to control, revealed by IF microscopy (H), and cell quantification indicated its

Figure 5. *Continued*

similarity to control in 9 and 60 dpi (I), with a preferential localization bias toward ONL than INL and GCL in VPA experimental regime compared with control (J); ANOVA test, *p < 0.01, **p < 0.02 in (J).

N = 6 biological replicates in all experiments. Scale bars, 10 μm in (B, E, and H). Error bars are SD. The asterisk marks the injury site in (B, E, and H). ONL, outer nuclear layer; INL, inner nuclear layer; GCL, ganglion cell layer. See also Figures S1–S4.

We further investigated, whether these newly formed MGPCs restore their functionality at a later stage of regeneration. For this, we labeled the newly formed MGPCs, after VPA withdrawal, with BrdU for 3 days. These BrdU cells were then traced up to 60 dpi and compared with those at 9 dpi in another similar experiment. The 9 dpi data would give us an idea about the approximate number of BrdU-positive cells that appeared in the retina after VPA withdrawal, which we then compared with the 60 dpi data. We found that the MGPCs migrated to various cell layers of the retina even at 60 dpi and showed only a marginal decline in cell number when compared with control, where there was no drug treatment (Figures 5G–5J).

Hdac-Her4.1 Axis Is Necessary for the Essential Cytokine Regulation during MGPCs Formation

Cytokines released at the site of injury trigger the regeneration cascade in the retina (Elsaeidi et al., 2014; Gramage et al., 2015; Wan et al., 2014; Zhao et al., 2014). We reasoned that the reintroduction of MGPCs after TSA/VPA withdrawal might involve the active participation of cytokines, as Hdacs could regulate them in other systems (Larsen et al., 2007; Leoni et al., 2005; Li et al., 2008). To decipher this, we first examined if regeneration-associated cytokines are affected by TSA/VPA treatment. We found that the majority of the cytokines like *il6*, *il11a*, *il11b*, *lepa*, *lepb*, and *crlf* and receptors like *il11ra*, *lepr*, and *lifra* were significantly inhibited in 2 dpi retina treated with TSA/VPA (Figures 6A and 6B), which may also explain the lack of enough MGPCs for regeneration. Moreover, these cytokines, which get upregulated in the injured retina, were downregulated with Hdacs' inhibition, revealed in a whole-retina RNA-seq analysis, at 4 dpi (Figure S6G and Table S1). We then investigated whether these cytokines possibly contribute to the reappearance of MGPCs and normal regeneration after withdrawal of Hdacs' inhibition. To address this, we designed an experimental timeline in which zebrafish were given TSA dip treatment from the time of injury till 4 dpi and shifted to fresh water for 2 more days and the eyes harvested at 6 dpi (Figure 6C). The cytokines showed a drastic increase, more than the normal levels found in 2 or 6 dpi retina (Figures 6D and 6E). We speculated whether the increased *her4.1* levels caused by TSA/VPA treatment contributed to the decline in the levels of cytokines, as a potential reason for reduced proliferation after retinal injury. *In silico* analysis revealed several Hes/Her binding sites (Kageyama et al., 2007) in the regulatory sequences of various cytokines addressed in this study (Figure S6H). We then decided to probe if this Her4.1-mediated repression exists on cytokine gene regulations in injured retina. We performed knockdown of *her4.1* at 3 dpi and analyzed the levels of cytokines at 5 dpi (Figure 6F). Interestingly, we found upregulation of almost all cytokines with the *her4.1* knockdown in the retina (Figure 6G). We reasoned that the Her4.1-mediated repression of cytokines could get relieved with TSA withdrawal. In a confirmative result, we found that the enhanced levels of *her4.1* with TSA/VPA treatment would decline progressively after the drug withdrawal (Figure 6H). This observation could be because of auto–negative feedback regulation of Her4.1 on its transcription (Figure 6I) (Wilson et al., 2016), similar to other Hes/Her proteins' auto-inhibitory regulations (Giudicelli et al., 2007; Hubaud and Pourquie, 2014). These results suggest that new injury is not necessary for the observed cytokine re-induction, as long as Her4.1 expression stays low after drug withdrawal. Furthermore, many regeneration-associated genes like *ascl1a*, *lin28a*, *mycb*, and *sox2* reappeared, probably influenced by the cytokines' surge (Figures 6J–6L), causing an overall standard regenerative response.

Hdacs Are Necessary for Normal Distribution of MGPCs Across Retina Layers

As we found the necessity of Hdacs in MGPCs formation, a similar mechanism presumably underlies progenitor differentiation and their migration. We then explored if Hdacs are necessary for the movement of MGPCs across various retinal layers. In an experiment, we labeled almost all MGPCs with BrdU from the time of injury to 5 dpi (Figure 7A). The fish were then exposed to VPA from 7 to 14 dpi, with an aim to block Hdacs during the cell migration/differentiation phase of retina regeneration. Although we found no apparent reduction in the total number of cells at 14 dpi, there was a preferential localization of the migrated cells to the outer nuclear layer, with a marginal decrease in the inner nuclear layer and a significant decline in the ganglion cell layer (Figures 7B and 7C). These findings suggest that Hdacs-driven gene regulation persists even at later phases of retina regeneration, which could influence the migration pattern of MGPCs to various retinal layers.

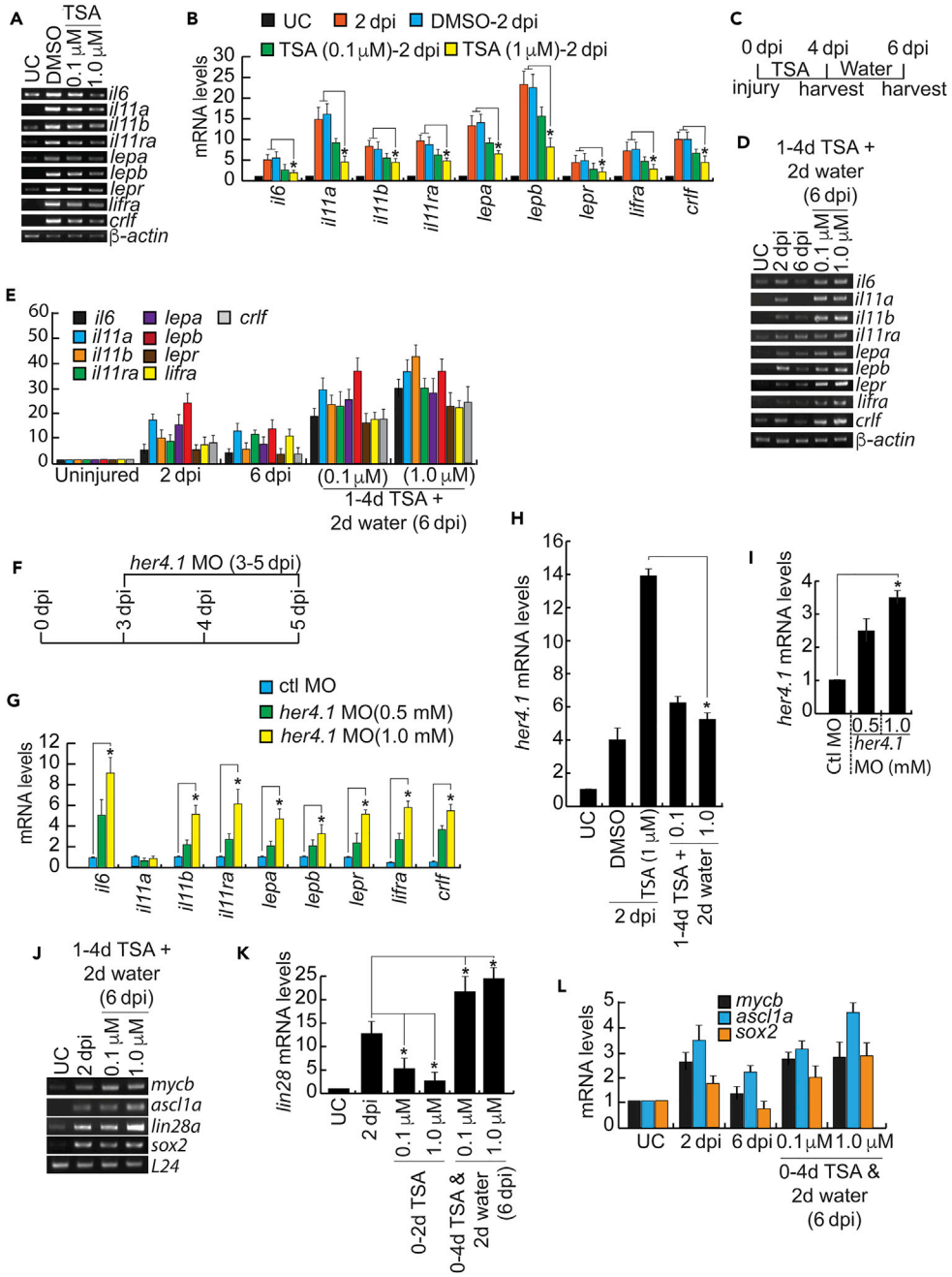

Figure 6. Hdac-Influenced MGPCs' Formation Is Mediated through Her4.1 Cytokine Axis

(A and B) RT-PCR (A) and qPCR (B) assay revealed injury-induced expression of cytokines in uninjured, 2 dpi, and TSA-treated 2 dpi retina; *p < 0.01 in (B), N = 6 biological replicates.

(C–E) Enhanced expression of cytokines in TSA withdrawal experiments as per the experimental timeline (C), shown by RT-PCR (D) and qPCR (E).

(F) Experimental timelines for late knockdown of *her4.1*, from 3–5 dpi.

(G) qPCR of various cytokines with 2 concentrations of *her4.1* MO electroporated as per experimental timeline in (F). *p<0.001.

(H) Downregulation of *her4.1* in TSA withdrawal experiments as per experimental timeline in (C); *p < 0.007.

(I) qPCR of *her4.1* with two concentrations of *her4.1* MO electroporated as per experimental timeline in (F); *p < 0.004.

(J–L) RT-PCR (J) and qPCR (K and L) were used to assay re-induction of injury-induced genes like *mycb*, *ascl1a*, *lin28a*, and *sox2* in uninjured, 2 dpi, and post-TSA treatment, which show significant upregulation of *lin28a* (K) and moderate increase in the level of other genes (L); ANOVA test, *p < 0.001 in (K).

N = 6 biological replicates in all. Error bars are SD. See also Figures S4–S6.

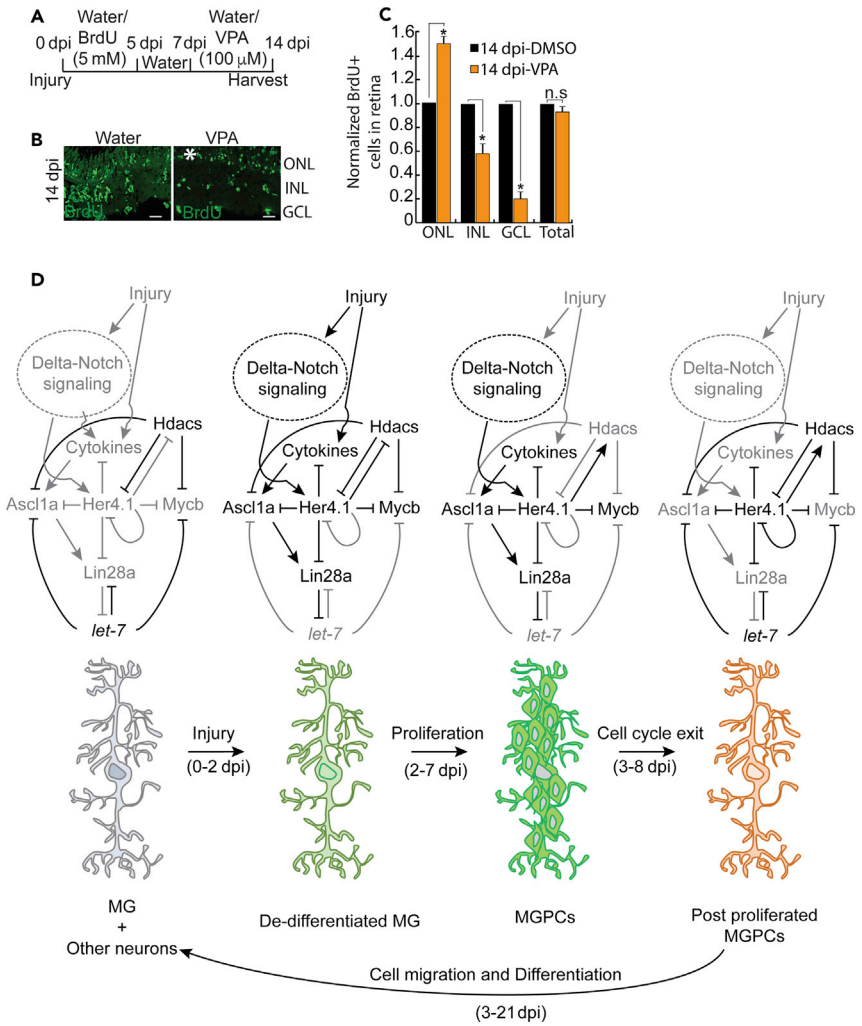

Figure 7. Hdacs' Inhibition Causes Selective Bias in MGPCs' Migration toward the Outer Nuclear Layer

(A–C) Determination of the fate of MGPCs in Hdac-inhibited condition as shown in experimental timeline (A), shows a significant increase of cell localization in ONL and a decline in INL and GCL, revealed by immunofluorescence (IF) microscopy (B) and quantified in (C), in the 14 dpi retina. *$p < 0.0004$ in (C), N = 6 biological replicates.

(D) Signaling pathways and genes that are regulated by Hdacs at different times and stages of retina regeneration.

Scale bar, 10 μm in (B). Error bars are SD. The asterisk marks the injury site in (B). ONL, outer nuclear layer; INL, inner nuclear layer; GCL, ganglion cell layer. See also Figures S4 and S6.

DISCUSSION

We explored the significance of HDACs, with a distinct focus on Hdac1, during retina regeneration and fin blastema formation in this study. Although the involvement of Hdac1 in progenitor differentiation is known during embryonic retinal development (Yamaguchi et al., 2005), proper cell division, and maintenance of pluripotency of embryonic stem (ES) cells (Jamaladdin et al., 2014), its mechanistic involvement during retina regeneration remained underexplored. Following injury, we found a drastic decline in the transcript levels of *hdac1* throughout the retina, which was restored back near MGPCs only at around 4 dpi. On the other hand, the protein level of Hdac1 remained unchanged in MGPCs and their neighboring cells until 4 dpi, a time when it stayed low in expression in MGPCs. Interestingly, at a later time point, 6 dpi, Hdac1 protein again become ubiquitous in all retinal cells. These seemingly contradictory observations regarding transcript and protein levels of Hdac1, found in our study, might hold the key to successful retina regeneration. The presence of Hdac1 protein in all retinal cells except MGPCs suggests the existence of Hdac1-mediated repression of regeneration-associated genes in these cells. Conversely, depletion of Hdac1 from MGPCs during proliferative phase ensures the reversal of this blockade of transcription as a necessity

for successful proliferation. The reappearance of Hdac1 and the subsequent inhibition of transcription of regeneration-associated genes in post-proliferated MGPCs suggest its role not only in potentiating MGPCs for successful cell multiplication brought about by its depletion but also in controlling the extent of proliferation at the vicinity of injury. In an analogous situation, HDAC1 in ES cells was reported to selectively target the promoters of pluripotency-inducing factors like Oct4, Sox2, and Nanog as a requirement for controlling their expression (Kidder and Palmer, 2012). Also, depletion of HDAC1 has been shown to cause enrichment of ES cell-specific gene expression. Similar necessary role of HDAC1 is also required for proper differentiation regime of ES cells (Dovey et al., 2010). Given the similarity between ES cells and MGPCs regarding gene expression, we speculate that the relocation of *hdac1* from its panretinal appearance to the neighboring cells of MGPCs probably would act similarly. Further studies are necessary to prove the guiding factors that regulate *hdac1* expression near MGPCs, and to find the collaborating factors that guide Hdac1 or other Hdacs to specific gene targets to regulate their expression.

Our study also supports another recently discovered phenomenon in mice retina, where the researchers over-expressed Ascl1 along with Hdac inhibition for promoting the regenerative capacity of mouse MG (Jorstad et al., 2017). It is interesting to note that in our zebrafish study too we find a global decline in *hdac1*, *hdac4*, *hdac7*, and *hdac9* mRNA levels soon after injury. Furthermore, the mRNA levels are restored back to normalcy, but actively proliferating MGPCs lacked Hdac1 protein, which indicates that its absence is a favorable criterion for normal cell proliferation. However, the panretinal decline in Hdac activity was not a facilitator of MGPCs proliferation in zebrafish, probably because of upregulated Her4.1 and downregulated *lin28a* levels.

We found that the global decline in expression of other *hdac* genes, namely, *hdac4*, *hdac7*, and *hdac9*, in post-injured retina are restored back to normalcy at later stages of regeneration. This phenomenon may potentially act as a prelude to unblock the transcriptional repression of various pro-proliferative genes like pluripotency-inducing factors to bring about successful regeneration. Since we found a good correlation between the effects of *hdac1* knockdown and pan-Hdacs inhibition using TSA/VPA in regenerating retina, we speculate that Hdac1 might be capable of subduing the activity of other Hdacs, similar to that reported in other systems (Lagger et al., 2002; Montgomery et al., 2007; Witt et al., 2009). Increase in the level of acetylated histone4 upon knocking down *hdac1* separately or inhibiting all Hdacs through TSA also could justify the overall increase in gene expression of regeneration-associated genes like *ascl1a*, *myca*, *mycb*, and *her4.1*. We further show that the abundance of *her4.1* could account for reduced MGPCs, as is evident from its knockdown in the proliferative phase of regeneration, causing a significant increase in the number of MGPCs.

It is believed that Delta-Notch signaling enables the retina to limit the zone of proliferation near the injury site. Now, considering that *hdac1* expression is predominant in the post-proliferative phase of MGPCs, it is logical to find upregulated expression of *hdac*s upon *her4.1* blockade. In other words, decline in *her4.1* because of DAPT treatment, causing an increased cell number, could bring about more cells that exit cell cycle, and hence would accompany an increased *hdacs* level.

It is interesting to note that, upon knocking down *hdac1* separately or inhibiting all Hdacs in general, the number of MGPCs decline drastically with a deleterious effect on retina regeneration. This scenario might be possible through a super-abundance of a repressor like *her4.1*, which we found had a substantial inhibitory effect on *lin28a*, which is a vital pluripotency-inducing factor. According to a previous study (Ramachandran et al., 2010a), a decrease in Lin28a would ensure the presence of high levels of *let-7* microRNA, which could prevent the translation of several regeneration-associated genes such as *ascl1a*, *mycb*, and *zic2b* and components of Sonic hedgehog signaling (Kaur et al., 2018; Ramachandran et al., 2010a). In support of this speculation, this study found that the panretinal Hdacs inhibition brought about an enhancement of *let-7* microRNA. Therefore, downregulation of *lin28a* and upregulation of *let-7* microRNA in the Hdacs-inhibited retina could repress the translation of *ascl1a* and *mycb*, despite their increased levels of mRNA, resulting in lack of adequate MGPCs formation. This part of the study also provides insights into the significance of depletion of Hdac1 in MGPCs, which in turn would regulate Her4.1 to induce Lin28a, which would be crucial for the successful proliferation of MGPCs.

Cytokine surge near the injury site often facilitates retinal regeneration (Goldman, 2014; Wan and Goldman, 2016). The involvement of cytokines is also prominent in other tissue regeneration (Bouzaffour

et al., 2009; Gonzalez-Rosa et al., 2017; Li et al., 2014), which makes the involvement of Hdacs-cytokines link crucial in retina-regeneration-specific gene expression paradigm. In general, the typical Hdacs expression necessitates the injury-induced cytokines as a prelude to successful regeneration, and their inhibition downregulates different regeneration-associated cytokines, thus culminating in reduced MGPCs proliferation. Withdrawal of the block on Hdacs function showed that the suspension of MGPCs proliferation by Hdacs inhibition was reversible, resulting in resumption of regeneration through a reappearance of cytokine surge and pluripotency factors like *lin28a*, which possibly is brought about by the disappearance of the abundant repressors like *her4.1*. This regulatory network could lead to the re-induction of MGPCs, which are BrdU-traceable even after 60 days.

The complex mechanism of temporal regulation of retina regeneration through Hdacs is presented in a model comprising the findings from this study (Figure 7D). In differentiated MG, the presence of Hdacs ensures blockade of transcription of pro-proliferative genes like *ascl1a* and *mycb*. The reported retinal abundance of *let-7* microRNA, which could block the translation of *ascl1a* and *mycb* also support this hypothesis (Ramachandran et al., 2010a). Upon injury, through different cellular signaling pathways, pro-proliferative genes like *ascl1a* are highly induced, which upregulates *lin28a*, which helps in degradation of *let-7* microRNA. Therefore, in de-differentiating MGs, even though Hdacs might be present, gene regulatory networks responsible for differentiation are already afoot ensuring the successful formation of MGPCs. At this stage, Delta/Notch-signaling-mediated induction of *her4.1* in the neighboring cells of MGPCs could be responsible for inhibiting *lin28a* transcription, thus controlling the extension of de-differentiation and proliferation. In this study, the *her4.1* knockdown in the proliferative phase of regeneration causes an increase in the MGPCs. In proliferating MGPCs, depletion of Her4.1 is also necessary for building up adequate levels of *lin28a* and cytokines. Furthermore, to control the extent of regeneration, Her4.1, which is a downstream target of Notch signaling, self-downregulates its expression (Wilson et al., 2016), thus allowing reappearance of Hdacs, which may bring about differentiation of newly generated cells. Finally, our study unravels essential mechanisms by which Hdacs orchestrate these effects through mutual signaling pathways yielded through a tight regulation of Her4.1-Lin28a axis bringing changes in the expression of several regeneration-associated genes and cytokines. This study places Hdacs among critical regulators required for tissue regeneration, providing valuable insights for understanding signaling mechanisms that might help in understanding MG reprogramming in the injured mammalian retina, and also regarding damaged human retinae toward successful repair.

Limitation of the Study

Absence of a well-characterized Her4.1 antibody for use in zebrafish limited a few experimental explorations in this study.

METHODS

All methods can be found in the accompanying Transparent Methods supplemental file.

SUPPLEMENTAL INFORMATION

Supplemental Information includes Transparent Methods, six figures, and three tables and can be found with this article online at https://doi.org/10.1016/j.isci.2018.08.008.

ACKNOWLEDGMENTS

S.M., M.A.K., M.C., R.A., A.J.K.– acknowledge their financial support from the Indian Institute of Science Education and Research, Mohali (IISER Mohali). P.S. acknowledges financial support from the Wellcome Trust/DBT India Alliance, India. S.K. acknowledges her financial support from the Department of Biotechnology (DBT), Ministry of Science and Technology, Govt. of India for Senior Research Fellowship. S.G. acknowledges her financial support from the Indian Council of Medical Research for Senior Research Fellowship. This work was supported by the Wellcome Trust/DBT India Alliance, India Intermediate Fellowship (IA/I/12/2/500630) awarded to R.R. R.R. also acknowledges extramural research funding from DBT India (102/IFD/SAN/3975/2015-2016), (102/IFD/SAN/2255/2017-2018) and intramural funding support from IISER Mohali, India.

The authors express their gratitude to Daniel Goldman, Molecular and Behavioral Neuroscience Institute and Department of Biological Chemistry, University of Michigan, USA, for sharing promoter clones of 1016 *tuba1a*, *lin28a*, *ascl1a*, and *insm1a* genes.

AUTHOR CONTRIBUTIONS

R.R. conceived the study and designed the experiments. S.M., P.S., and S.K. performed the majority of experiments. S.K. and P.S. contributed equally to this work. R.A., M.A.K., S.G., and M.C. performed a few critical RNA *in situ* hybridizations, immunofluorescence microscopy, and cell count experiments. R.R., S.M., P.S., and S.K. analyzed the data. A.J.K. performed the retinal cell sorting. R.R. wrote the manuscript with critical inputs from S.M., M.C., and S.G.

DECLARATION OF INTERESTS

The authors declare no competing financial interests.

Received: March 20, 2018
Revised: July 18, 2018
Accepted: August 10, 2018
Published: September 28, 2018

REFERENCES

Ail, D., and Perron, M. (2017). Retinal degeneration and regeneration-lessons from fishes and amphibians. Curr. Pathobiol. Rep. *5*, 67–78.

Bolden, J.E., Peart, M.J., and Johnstone, R.W. (2006). Anticancer activities of histone deacetylase inhibitors. Nat. Rev. Drug Discov. *5*, 769–784.

Bologna-Molina, R., Mosqueda-Taylor, A., Molina-Frechero, N., Mori-Estevez, A.D., and Sanchez-Acuna, G. (2013). Comparison of the value of PCNA and Ki-67 as markers of cell proliferation in ameloblastic tumors. Med. Oral Patol. Oral Cir. Bucal *18*, e174–e179.

Bouzaffour, M., Dufourcq, P., Lecaudey, V., Haas, P., and Vriz, S. (2009). Fgf and Sdf-1 pathways interact during zebrafish fin regeneration. PLoS One *4*, e5824.

Bringmann, A., Iandiev, I., Pannicke, T., Wurm, A., Hollborn, M., Wiedemann, P., Osborne, N.N., and Reichenbach, A. (2009). Cellular signaling and factors involved in Muller cell gliosis: neuroprotective and detrimental effects. Prog. Retin. Eye Res. *28*, 423–451.

Conner, C., Ackerman, K.M., Lahne, M., Hobgood, J.S., and Hyde, D.R. (2014). Repressing notch signaling and expressing TNFalpha are sufficient to mimic retinal regeneration by inducing Müller glial proliferation to generate committed progenitor cells. J. Neurosci. *34*, 14403–14419.

Dovey, O.M., Foster, C.T., and Cowley, S.M. (2010). Histone deacetylase 1 (HDAC1), but not HDAC2, controls embryonic stem cell differentiation. Proc. Natl. Acad. Sci. USA *107*, 8242–8247.

Elsaeidi, F., Bemben, M.A., Zhao, X.F., and Goldman, D. (2014). Jak/Stat signaling stimulates zebrafish optic nerve regeneration and overcomes the inhibitory actions of Socs3 and Sfpq. J. Neurosci. *34*, 2632–2644.

Elsaeidi, F., Macpherson, P., Mills, E.A., Jui, J., Flannery, J.G., and Goldman, D. (2018). Notch suppression collaborates with Ascl1 and Lin28 to unleash a regenerative response in fish retina, but not in mice. J. Neurosci. *38*, 2246–2261.

Fausett, B.V., and Goldman, D. (2006). A role for alpha1 tubulin-expressing Müller glia in regeneration of the injured zebrafish retina. J. Neurosci. *26*, 6303–6313.

Gemberling, M., Bailey, T.J., Hyde, D.R., and Poss, K.D. (2013). The zebrafish as a model for complex tissue regeneration. Trends Genet. *29*, 611–620.

Giudicelli, F., Ozbudak, E.M., Wright, G.J., and Lewis, J. (2007). Setting the tempo in development: an investigation of the zebrafish somite clock mechanism. PLoS Biol. *5*, e150.

Goldman, D. (2014). Müller glial cell reprogramming and retina regeneration. Nat. Rev. Neurosci. *15*, 431–442.

Gonzalez-Rosa, J.M., Burns, C.E., and Burns, C.G. (2017). Zebrafish heart regeneration: 15 years of discoveries. Regeneration (Oxf) *4*, 105–123.

Gorsuch, R.A., Lahne, M., Yarka, C.E., Petravick, M.E., Li, J., and Hyde, D.R. (2017). Sox2 regulates Müller glia reprogramming and proliferation in the regenerating zebrafish retina via Lin28 and Ascl1a. Exp. Eye Res. *161*, 174–192.

Gramage, E., D'Cruz, T., Taylor, S., Thummel, R., and Hitchcock, P.F. (2015). Midkine-a protein localization in the developing and adult retina of the zebrafish and its function during photoreceptor regeneration. PLoS One *10*, e0121789.

Gregoretti, I.V., Lee, Y.M., and Goodson, H.V. (2004). Molecular evolution of the histone deacetylase family: functional implications of phylogenetic analysis. J. Mol. Biol. *338*, 17–31.

Huang, Y., Myers, S.J., and Dingledine, R. (1999). Transcriptional repression by REST: recruitment of Sin3A and histone deacetylase to neuronal genes. Nat. Neurosci. *2*, 867–872.

Hubaud, A., and Pourquie, O. (2014). Signalling dynamics in vertebrate segmentation. Nat. Rev. Mol. Cell Biol. *15*, 709–721.

Jamaladdin, S., Kelly, R.D., O'Regan, L., Dovey, O.M., Hodson, G.E., Millard, C.J., Portolano, N., Fry, A.M., Schwabe, J.W., and Cowley, S.M. (2014). Histone deacetylase (HDAC) 1 and 2 are essential for accurate cell division and the pluripotency of embryonic stem cells. Proc. Natl. Acad. Sci. USA *111*, 9840–9845.

Jorstad, N.L., Wilken, M.S., Grimes, W.N., Wohl, S.G., VandenBosch, L.S., Yoshimatsu, T., Wong, R.O., Rieke, F., and Reh, T.A. (2017). Stimulation of functional neuronal regeneration from Müller glia in adult mice. Nature *548*, 103–107.

Kageyama, R., Ohtsuka, T., and Kobayashi, T. (2007). The Hes gene family: repressors and oscillators that orchestrate embryogenesis. Development *134*, 1243–1251.

Kaur, S., Gupta, S., Chaudhary, M., Khursheed, M.A., Mitra, S., Kurup, A.J., and Ramachandran, R. (2018). let-7 MicroRNA-mediated regulation of Shh signaling and the gene regulatory network is essential for retina regeneration. Cell Rep. *23*, 1409–1423.

Kidder, B.L., and Palmer, S. (2012). HDAC1 regulates pluripotency and lineage specific transcriptional networks in embryonic and trophoblast stem cells. Nucleic Acids Res. *40*, 2925–2939.

Kimmel, R.A., and Meyer, D. (2010). Molecular regulation of pancreas development in zebrafish. Methods Cell Biol. *100*, 261–280.

Kyritsis, N., Kizil, C., Zocher, S., Kroehne, V., Kaslin, J., Freudenreich, D., Iltzsche, A., and Brand, M. (2012). Acute inflammation initiates the regenerative response in the adult zebrafish brain. Science *338*, 1353–1356.

Lagger, G., O'Carroll, D., Rembold, M., Khier, H., Tischler, J., Weitzer, G., Schuettengruber, B., Hauser, C., Brunmeir, R., Jenuwein, T., et al. (2002). Essential function of histone deacetylase 1 in proliferation control and CDK inhibitor repression. EMBO J. *21*, 2672–2681.

Larsen, L., Tonnesen, M., Ronn, S.G., Storling, J., Jorgensen, S., Mascagni, P., Dinarello, C.A., Billestrup, N., and Mandrup-Poulsen, T. (2007). Inhibition of histone deacetylases prevents cytokine-induced toxicity in beta cells. Diabetologia *50*, 779–789.

Leoni, F., Fossati, G., Lewis, E.C., Lee, J.K., Porro, G., Pagani, P., Modena, D., Moras, M.L., Pozzi, P.,

Reznikov, L.L., et al. (2005). The histone deacetylase inhibitor ITF2357 reduces production of pro-inflammatory cytokines in vitro and systemic inflammation in vivo. Mol. Med. *11*, 1–15.

Li, N., Wang, C., Jia, L., and Du, J. (2014). Heart regeneration, stem cells, and cytokines. Regen. Med. Res. *2*, 6.

Li, N., Zhao, D., Kirschbaum, M., Zhang, C., Lin, C.L., Todorov, I., Kandeel, F., Forman, S., and Zeng, D. (2008). HDAC inhibitor reduces cytokine storm and facilitates induction of chimerism that reverses lupus in anti-CD3 conditioning regimen. Proc. Natl. Acad. Sci. USA *105*, 4796–4801.

Lombardi, P.M., Cole, K.E., Dowling, D.P., and Christianson, D.W. (2011). Structure, mechanism, and inhibition of histone deacetylases and related metalloenzymes. Curr. Opin. Struct. Biol. *21*, 735–743.

Luo, J., Uribe, R.A., Hayton, S., Calinescu, A.A., Gross, J.M., and Hitchcock, P.F. (2012). Midkine-A functions upstream of Id2a to regulate cell cycle kinetics in the developing vertebrate retina. Neural Dev. *7*, 33.

Mandyam, C.D., Harburg, G.C., and Eisch, A.J. (2007). Determination of key aspects of precursor cell proliferation, cell cycle length and kinetics in the adult mouse subgranular zone. Neuroscience *146*, 108–122.

Mokalled, M.H., Patra, C., Dickson, A.L., Endo, T., Stainier, D.Y., and Poss, K.D. (2016). Injury-induced ctgfa directs glial bridging and spinal cord regeneration in zebrafish. Science *354*, 630–634.

Montgomery, R.L., Davis, C.A., Potthoff, M.J., Haberland, M., Fielitz, J., Qi, X., Hill, J.A., Richardson, J.A., and Olson, E.N. (2007). Histone deacetylases 1 and 2 redundantly regulate cardiac morphogenesis, growth, and contractility. Genes Dev. *21*, 1790–1802.

Munderloh, C., Solis, G.P., Bodrikov, V., Jaeger, F.A., Wiechers, M., Malaga-Trillo, E., and Stuermer, C.A. (2009). Reggies/flotillins regulate retinal axon regeneration in the zebrafish optic nerve and differentiation of hippocampal and N2a neurons. J. Neurosci. *29*, 6607–6615.

Nelson, C.M., Gorsuch, R.A., Bailey, T.J., Ackerman, K.M., Kassen, S.C., and Hyde, D.R. (2012). Stat3 defines three populations of Müller glia and is required for initiating maximal Müller glia proliferation in the regenerating zebrafish retina. J. Comp. Neurol. *520*, 4294–4311.

Poss, K.D., Wilson, L.G., and Keating, M.T. (2002). Heart regeneration in zebrafish. Science *298*, 2188–2190.

Powell, C., Elsaeidi, F., and Goldman, D. (2012). Injury-dependent Müller glia and ganglion cell reprogramming during tissue regeneration requires Apobec2a and Apobec2b. J. Neurosci. *32*, 1096–1109.

Powell, C., Grant, A.R., Cornblath, E., and Goldman, D. (2013). Analysis of DNA methylation reveals a partial reprogramming of the Müller glia genome during retina regeneration. Proc. Natl. Acad. Sci. USA *110*, 19814–19819.

Rabinowitz, J.S., Robitaille, A.M., Wang, Y., Ray, C.A., Thummel, R., Gu, H., Djukovic, D., Raftery, D., Berndt, J.D., and Moon, R.T. (2017). Transcriptomic, proteomic, and metabolomic landscape of positional memory in the caudal fin of zebrafish. Proc. Natl. Acad. Sci. USA *114*, E717–E726.

Ramachandran, R., Fausett, B.V., and Goldman, D. (2010a). Ascl1a regulates Müller glia dedifferentiation and retinal regeneration through a Lin-28-dependent, let-7 microRNA signalling pathway. Nat. Cell Biol. *12*, 1101–1107.

Ramachandran, R., Reifler, A., Parent, J.M., and Goldman, D. (2010b). Conditional gene expression and lineage tracing of tuba1a expressing cells during zebrafish development and retina regeneration. J. Comp. Neurol. *518*, 4196–4212.

Ramachandran, R., Reifler, A., Wan, J., and Goldman, D. (2012a). Application of Cre-loxP recombination for lineage tracing of adult zebrafish retinal stem cells. Methods Mol. Biol. *884*, 129–140.

Ramachandran, R., Zhao, X.F., and Goldman, D. (2011). Ascl1a/Dkk/beta-catenin signaling pathway is necessary and glycogen synthase kinase-3beta inhibition is sufficient for zebrafish retina regeneration. Proc. Natl. Acad. Sci. USA *108*, 15858–15863.

Ramachandran, R., Zhao, X.F., and Goldman, D. (2012b). Insm1a-mediated gene repression is essential for the formation and differentiation of Müller glia-derived progenitors in the injured retina. Nat. Cell Biol. *14*, 1013–1023.

Reyes-Aguirre, L.I., and Lamas, M. (2016). Oct4 methylation-mediated silencing as an epigenetic barrier preventing müller glia dedifferentiation in a murine model of retinal injury. Front. Neurosci. *10*, 523.

Russell, C. (2003). The roles of hedgehogs and fibroblast growth factors in eye development and retinal cell rescue. Vision Res. *43*, 899–912.

Sherpa, T., Fimbel, S.M., Mallory, D.E., Maaswinkel, H., Spritzer, S.D., Sand, J.A., Li, L., Hyde, D.R., and Stenkamp, D.L. (2008). Ganglion cell regeneration following whole-retina destruction in zebrafish. Dev. Neurobiol. *68*, 166–181.

Singh, S.P., Holdway, J.E., and Poss, K.D. (2012). Regeneration of amputated zebrafish fin rays from de novo osteoblasts. Dev. Cell *22*, 879–886.

Thummel, R., Enright, J.M., Kassen, S.C., Montgomery, J.E., Bailey, T.J., and Hyde, D.R. (2010). Pax6a and Pax6b are required at different points in neuronal progenitor cell proliferation during zebrafish photoreceptor regeneration. Exp. Eye Res. *90*, 572–582.

Wan, J., and Goldman, D. (2016). Retina regeneration in zebrafish. Curr. Opin. Genet. Dev. *40*, 41–47.

Wan, J., Ramachandran, R., and Goldman, D. (2012). HB-EGF is necessary and sufficient for Müller glia dedifferentiation and retina regeneration. Dev. Cell *22*, 334–347.

Wan, J., Zhao, X.F., Vojtek, A., and Goldman, D. (2014). Retinal injury, growth factors, and cytokines converge on beta-catenin and pStat3 signaling to stimulate retina regeneration. Cell Rep. *9*, 285–297.

Wilson, S.G., Wen, W., Pillai-Kastoori, L., and Morris, A.C. (2016). Tracking the fate of her4 expressing cells in the regenerating retina using her4:Kaede zebrafish. Exp. Eye Res. *145*, 75–87.

Witt, O., Deubzer, H.E., Milde, T., and Oehme, I. (2009). HDAC family: what are the cancer relevant targets? Cancer Lett. *277*, 8–21.

Xu, W.S., Parmigiani, R.B., and Marks, P.A. (2007). Histone deacetylase inhibitors: molecular mechanisms of action. Oncogene *26*, 5541–5552.

Yamaguchi, M., Tonou-Fujimori, N., Komori, A., Maeda, R., Nojima, Y., Li, H., Okamoto, H., and Masai, I. (2005). Histone deacetylase 1 regulates retinal neurogenesis in zebrafish by suppressing Wnt and Notch signaling pathways. Development *132*, 3027–3043.

Zhao, X.F., Wan, J., Powell, C., Ramachandran, R., Myers, M.G., Jr., and Goldman, D. (2014). Leptin and IL-6 family cytokines synergize to stimulate Müller glia reprogramming and retina regeneration. Cell Rep. *9*, 272–284.

ISCI, Volume *7*

Supplemental Information

Histone Deacetylase-Mediated Müller Glia Reprogramming through Her4.1-Lin28a Axis Is Essential for Retina Regeneration in Zebrafish

Soumitra Mitra, Poonam Sharma, Simran Kaur, Mohammad Anwar Khursheed, Shivangi Gupta, Riya Ahuja, Akshai J. Kurup, Mansi Chaudhary, and Rajesh Ramachandran

Supplemental Figures
Figure S1

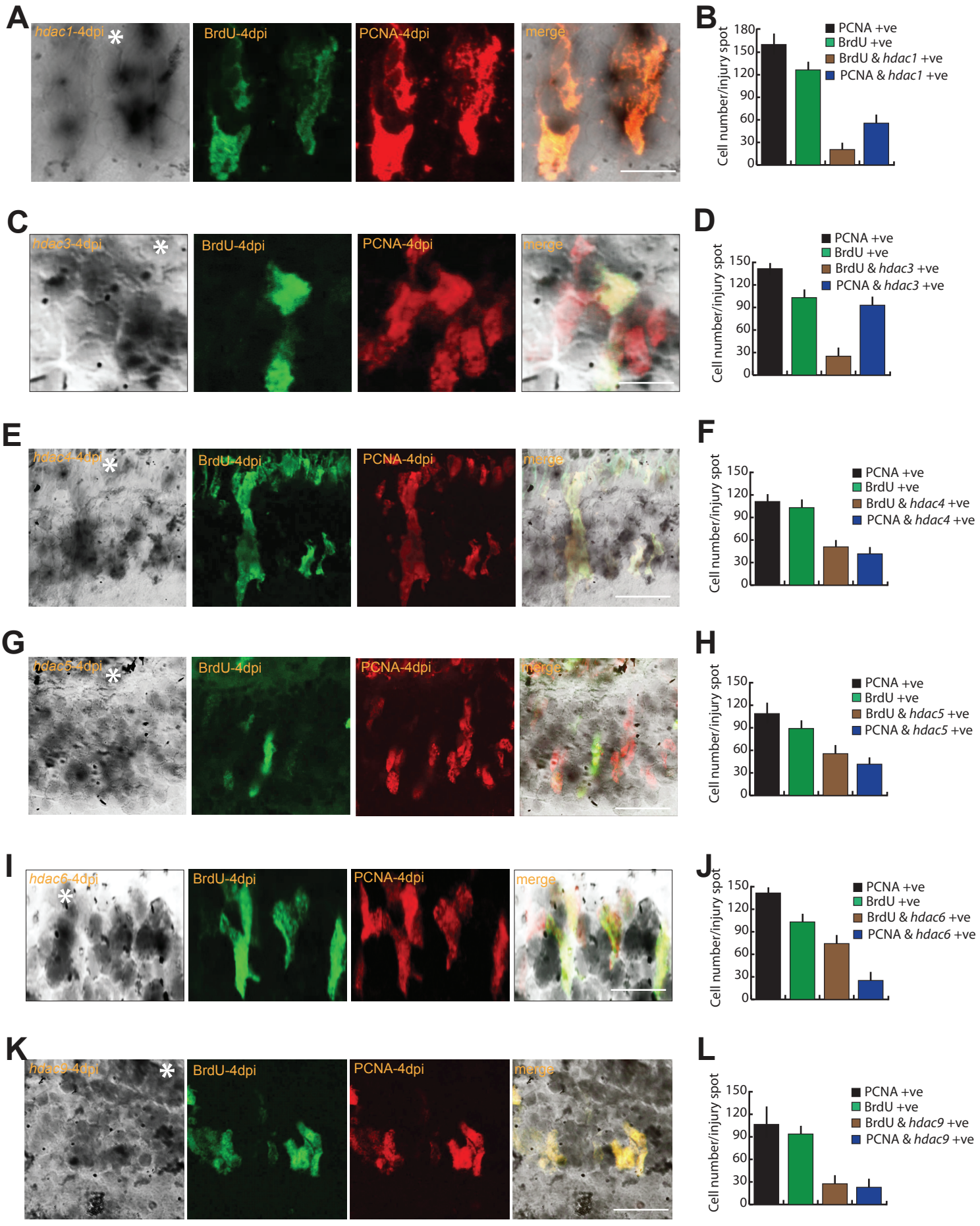

Figure S1: Spatial expression pattern of *hdac* genes in the retina. Related to Figure 1 and Figure 5.

(**A-L**) ISH of *hdac*s and IF microscopy of $BrdU^+/PCNA^+$ cells reveal that only a subpopulation of proliferating cells show expression of *hdac1* (**A, B**), *hdac3* (**C, D**), *hdac4* (**E, F**), *hdac5* (**G, H**), *hdac6* (**I, J**), and *hdac9* (**K, L**) in 4dpi retina. Scale bars, 10 µm (**A,C,E,G,I,K**). N = 6 biological replicates. Error bars are s.d. The asterisk marks the injury site in all.

Figure S2

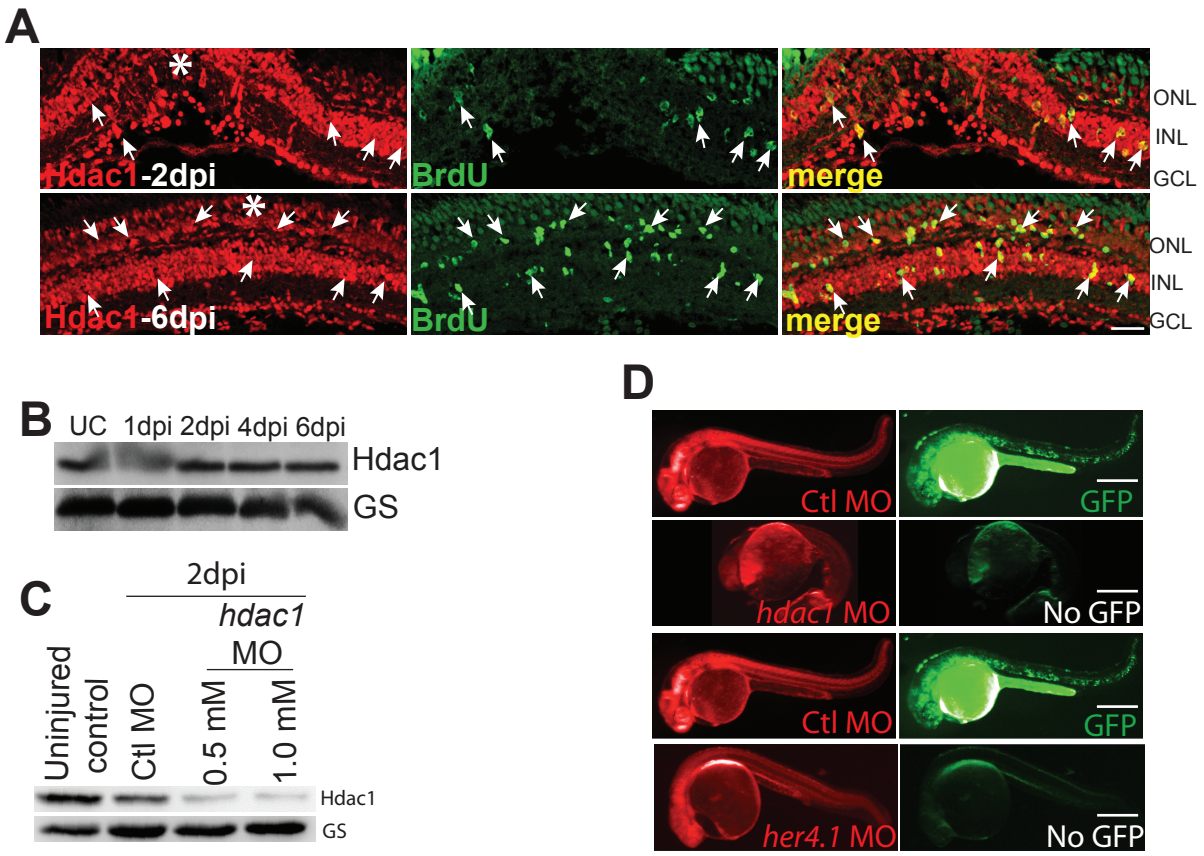
A
Hdac1-2dpi
BrdU
merge
ONL
INL
GCL
Hdac1-6dpi
BrdU
merge
ONL
INL
GCL
B
UC 1dpi 2dpi 4dpi 6dpi
Hdac1
GS
C
2dpi
hdac1 MO
Uninjured control
Ctl MO
0.5 mM
1.0 mM
Hdac1
GS
D
Ctl MO
GFP
hdac1 MO
No GFP
Ctl MO
GFP
her4.1 MO
No GFP
E
2dpi
Ctl MO (1mM)
hdac1 MO (0.5mM)
hdac1 MO (1mM)
2-hdac1 MO (0.5mM)
2-hdac1 MO (1mM)
Lissamine
PCNA
merge
ONL
INL
GCL
F
1.0mM
0.5mM
1mM
Normalized PCNA + cell number
1.0
0.8
0.6
0.4
0.2
0
Ctl MO
hdac1 MO
2-hdac1 MO

Figure S2: Hdac1 expression, its knockdown, MO efficiency, and its influence on cell proliferation. Related to Figure 1, Figure 2, Figure 4, and Figure 5.
(**A**) IF microscopy of Hdac1 at 2 and 6dpi retina along with $BrdU^{+}$ cells. (**B**) Expression pattern of Hdac1 protein at various times post-retinal injury by western blot analysis. GS-Glutamine synthetase, which is the loading control. (**C**) Western blot analysis of Hdac1, in *hdac1* MO electroporated retina at 2dpi, reveals specific blockade of its mRNA translation. GS-Glutamine synthetase. (**D**) Fluorescence images of 24hpf zebrafish embryos co-injected with control or gene-specific morpholinos and *gfp* mRNA appended with MO binding sequences, at the single cell stage. MOs used were 0.5mM each, in all experiments. (**E, F**) MO-based *hdac1* knockdown decreases $PCNA^{+}$ cells, relative to the control MO (**E**), which accounts for 80% reduction in cell number (**F**) in 2 dpi retina, ANOVA test, $^{*}P<0.002$. Scale bars, 10 μm (**A, E**), and 500 μm (**D**). N = 6 biological replicates. Error bars are s.d. The asterisk marks the injury site in all.

Figure S3

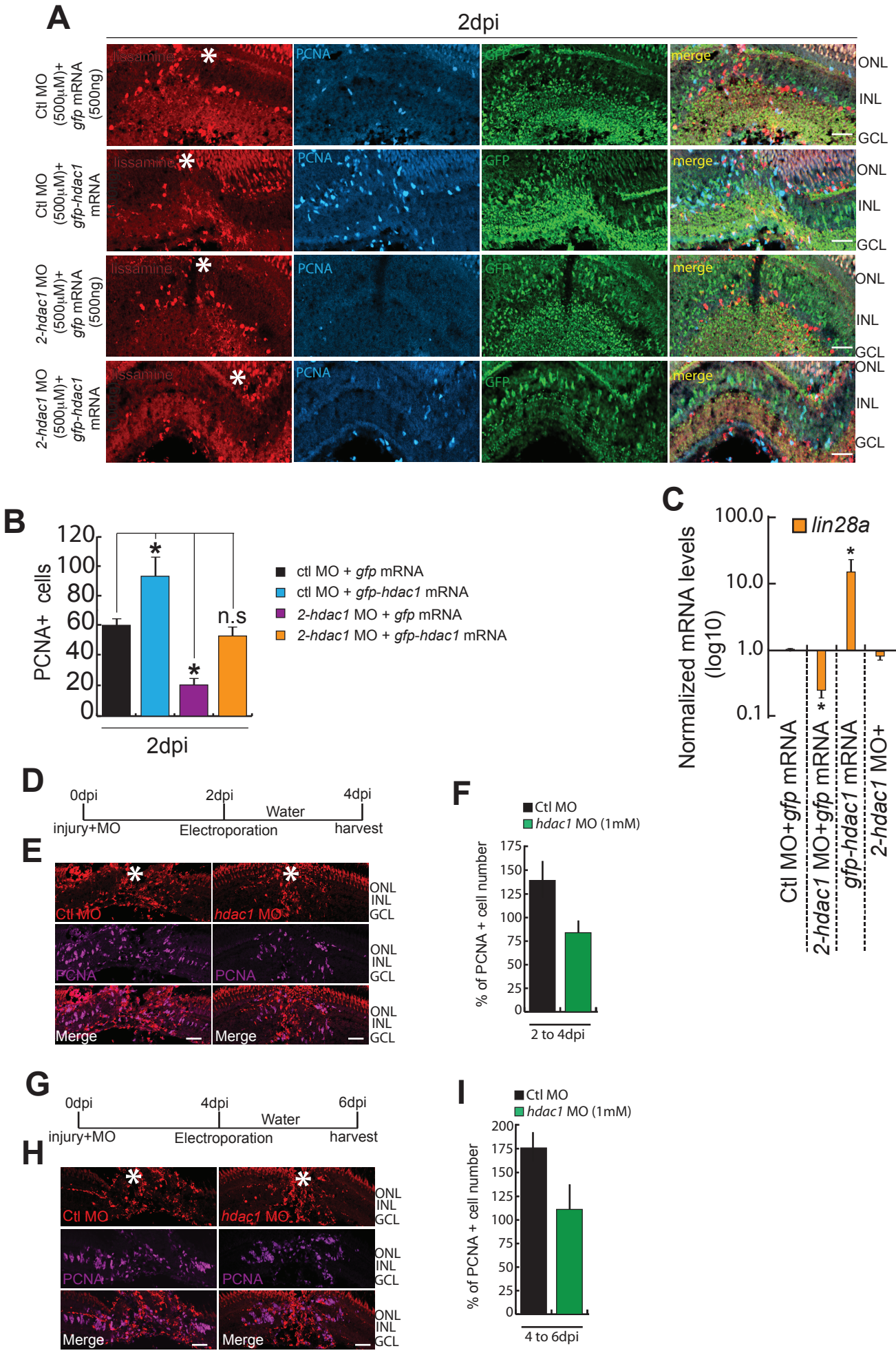
A
2dpi
Ctl MO (500µM)+ gfp mRNA (500ng)
Ctl MO (500µM)+ gfp-hdac1 mRNA
2-hdac1 MO (500µM)+ gfp mRNA (500ng)
2-hdac1 MO (500µM)+ gfp-hdac1 mRNA
lissamine
PCNA
GFP
merge
ONL
INL
GCL
B
PCNA+ cells
120
100
80
60
40
20
0
n.s
2dpi
ctl MO + gfp mRNA
ctl MO + gfp-hdac1 mRNA
2-hdac1 MO + gfp mRNA
2-hdac1 MO + gfp-hdac1 mRNA
C
Normalized mRNA levels (log10)
100.0
10.0
1.0
0.1
lin28a
Ctl MO+gfp mRNA
2-hdac1 MO+gfp mRNA
gfp-hdac1 mRNA
2-hdac1 MO+ gfp-hdac1 mRNA
D
0dpi
2dpi
4dpi
Water
injury+MO
Electroporation
harvest
E
Ctl MO
hdac1 MO
PCNA
Merge
ONL
INL
GCL
F
Ctl MO
hdac1 MO (1mM)
% of PCNA + cell number
175
150
125
100
75
50
25
0
2 to 4dpi
G
0dpi
4dpi
6dpi
Water
injury+MO
Electroporation
harvest
H
Ctl MO
hdac1 MO
PCNA
Merge
ONL
INL
GCL
I
Ctl MO
hdac1 MO (1mM)
% of PCNA + cell number
200
175
150
125
100
75
50
25
0
4 to 6dpi

Figure S3: The *hdac1* knockdown and its rescue. Related to Figure 3, Figure 4 and Figure 5.

(**A, B**) IF microscopy of retinal sections reveals the decrease in the number of $PCNA^{+}$ cells by morpholino-mediated *hdac1* knockdown at 2dpi during regeneration, which is rescued by *in situ hdac1* mRNA transfection (**A**), which is quantified (**B**). $^{*}P<0.004$, N = 4 biological replicates. (**C**). qPCR analysis of *lin28a* mRNA in 2dpi retina transfected/electroporated with control MO, *2-hdac1* MO with or without *gfp-hdac1* fusion mRNA. $^{*}P<0.002$. The results show that, (i) *lin28a* levels decline with repressed Hdac1 activity, (ii) *lin28a* is upregulated with *hdac1* transfection, (iii) the decline in *lin28a* levels because of *hdac1* repression is rescued by *hdac1* mRNA. (**D-I**) Late electroporation of *hdac1* MO (1mM) with an experiment timeline (**D, G**), and IF microscopy of retinal sections for PCNA and lissamine at 4dpi and 6dpi respectively (**E, H**), which is quantified (**F, I**), showing a reduction in cell proliferation. Scale bars, 10 μm (**A, E, H**). N = 6 biological replicates. Error bars are s.d. The asterisk marks the injury site in all.

Figure S4

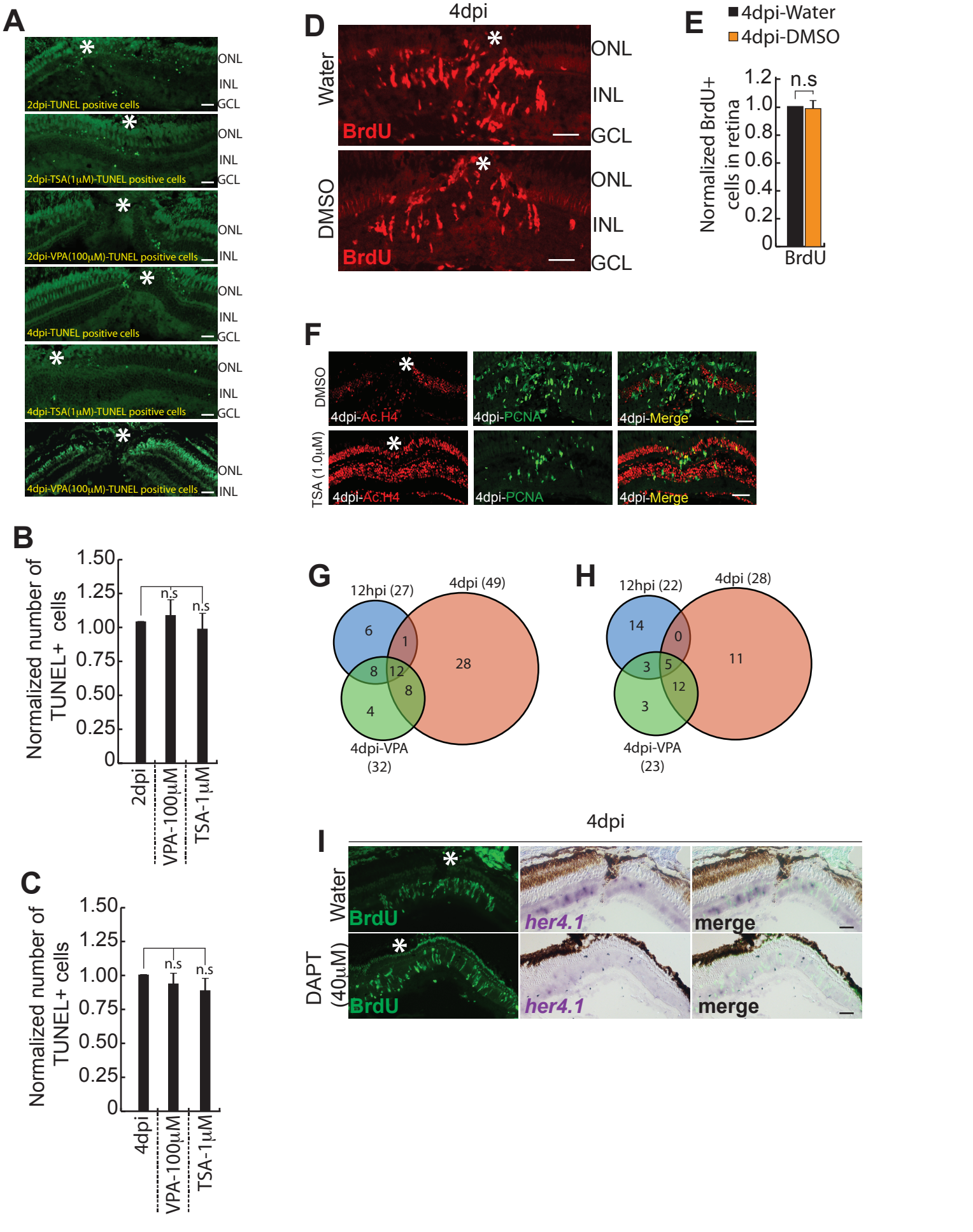
A
2dpi-TUNEL positive cells
2dpi-TSA(1μM)-TUNEL positive cells
2dpi-VPA(100μM)-TUNEL positive cells
4dpi-TUNEL positive cells
4dpi-TSA(1μM)-TUNEL positive cells
4dpi-VPA(100μM)-TUNEL positive cells
ONL
INL
GCL
B
Normalized number of TUNEL+ cells
1.50
1.25
1.00
0.75
0.50
0.25
0
n.s
n.s
2dpi
VPA-100μM
TSA-1μM
C
Normalized number of TUNEL+ cells
1.50
1.25
1.00
0.75
0.50
0.25
0
n.s
n.s
4dpi
VPA-100μM
TSA-1μM
D
4dpi
Water
DMSO
BrdU
ONL
INL
GCL
E
4dpi-Water
4dpi-DMSO
Normalized BrdU+ cells in retina
1.2
1.0
0.8
0.6
0.4
0.2
0
n.s
BrdU
F
DMSO
TSA (1.0μM)
4dpi-Ac.H4
4dpi-PCNA
4dpi-Merge
G
12hpi (27)
4dpi (49)
6
1
28
8
12
8
4
4dpi-VPA (32)
H
12hpi (22)
4dpi (28)
14
0
11
3
5
12
3
4dpi-VPA (23)
I
4dpi
Water
DAPT (40μM)
BrdU
her4.1
merge

Figure S4: TUNEL assay, Ac.H4 and global change in gene expression by RNAseq with TSA/VPA treatments. Related to Figure 2, Figure 3, Figure 4, Figure 5, Figure 6 and Figure 7.

(**A-C**) TUNEL assay seen by IF microscopy does not reveal an increased number of apoptotic cells, in Hdac blocked retinae at 2dpi and 4dpi (**A**) which are quantified (**B, C**). n.s=not significant. (**D, E**) $BrdU^+$ MGPCs in 4dpi retina do not significantly vary in number between DMSO treated and non-treated groups which are quantified (**E**), N = 4 biological replicates. (**F**) The IF microscopy shows increased Ac.H4 and decreased $PCNA^+$ MGPCs in TSA treated retina compared to control. (**G, H**) Venn diagrams representing the total number of transcription factors that are upregulated (**G**), and downregulated (**H**) with Hdac inhibition using VPA at 4dpi, which are normalized to uninjured and compared to 12hpi and 4dpi retina. Numbers outside the circles represent total transcription factors for the particular time point; inside circle represent unique and overlapping genes in **G** and **H**. (**I**) BF microscopic images of retina showing declined *her4.1* mRNA levels revealed in an ISH, after DAPT treatment. Scale bars, 10 μm (**A,D,F,I**). Error bars are s.d. The asterisk marks the injury site in all.

Figure S5

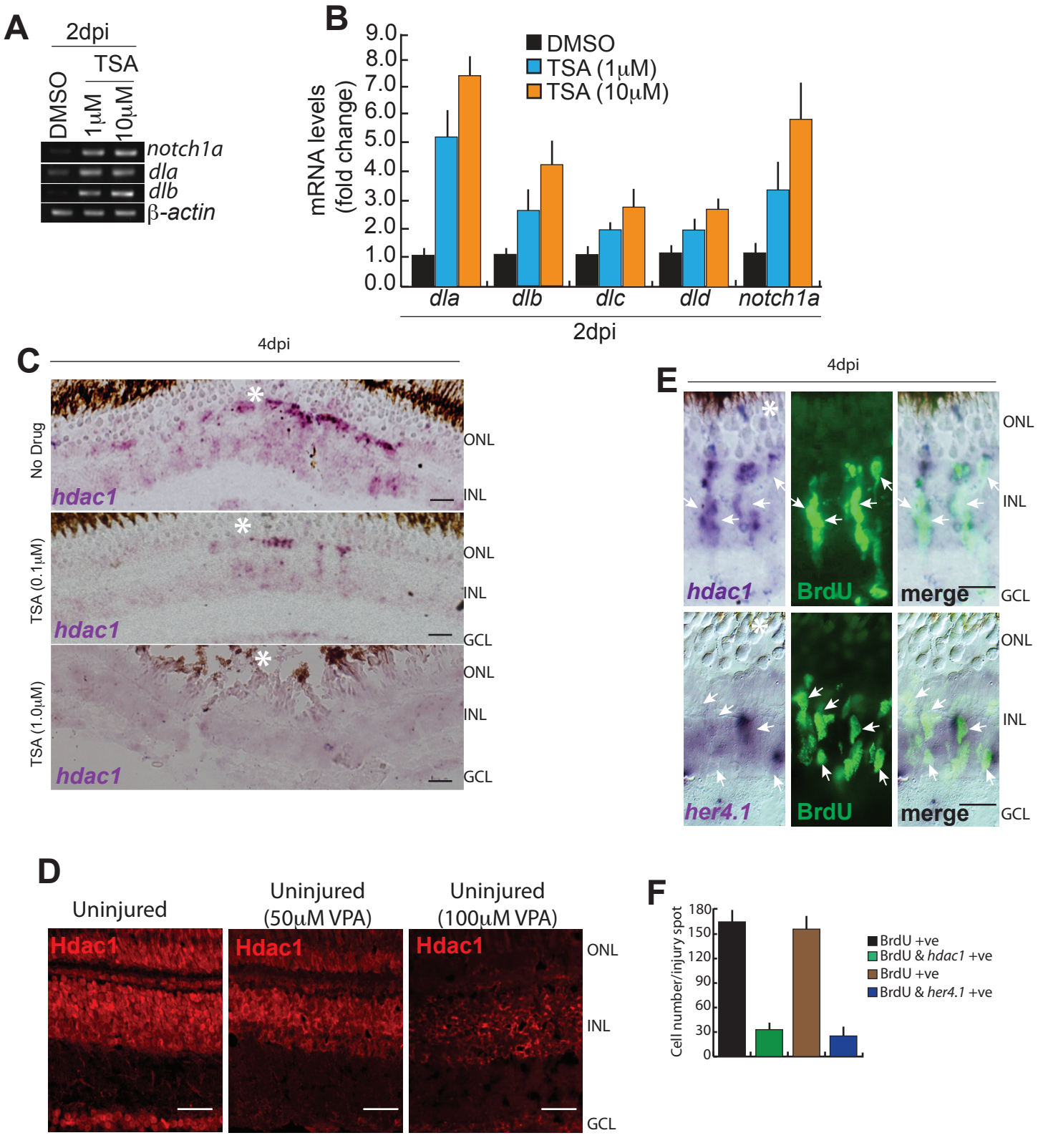
A
2dpi
TSA
DMSO
1μM
10μM
notch1a
dla
dlb
β-actin
B
mRNA levels (fold change)
9.0
8.0
7.0
6.0
5.0
4.0
3.0
2.0
1.0
0.0
DMSO
TSA (1μM)
TSA (10μM)
dla
dlb
dlc
dld
notch1a
2dpi
C
4dpi
No Drug
TSA (0.1μM)
TSA (1.0μM)
hdac1
ONL
INL
GCL
D
Uninjured
Uninjured (50μM VPA)
Uninjured (100μM VPA)
Hdac1
ONL
INL
GCL
E
4dpi
hdac1
BrdU
merge
her4.1
ONL
INL
GCL
F
Cell number/injury spot
180
150
120
90
60
30
0
BrdU +ve
BrdU & hdac1 +ve
BrdU +ve
BrdU & her4.1 +ve

Figure S5: Effect of Hdacs' inhibition on *hdac1* mRNA /Protein and Delta-Notch signaling components. Related to Figure 3, Figure 4, and Figure 6.

(**A, B**) RT-PCR (**A**), and qPCR (**B**) analysis of Notch signaling components reveal significant upregulation of *delta* and *notch* with Hdacs inhibition using TSA, at 2dpi. (**C**) BF microscopy images of *hdac1* mRNA ISH in cross sections of retina treated with TSA at 4dpi. (**D**) Microscopy images of Hdac1 IF of uninjured retinal cross-sections treated with VPA for 2 days. (**E, F**) BF microscopy images of *hdac1* and *her4.1* mRNA ISH and pulse labeled BrdU revealed by IF in retinal cross sections at 4dpi. Arrows indicate $BrdU^{+}$ but gene negative cells which are quantified (**F**). N = 6 biological replicates. Scale bars, 10 μm (**A, B, E**). Error bars are s.d. The asterisk marks the injury site in all.

Figure S6

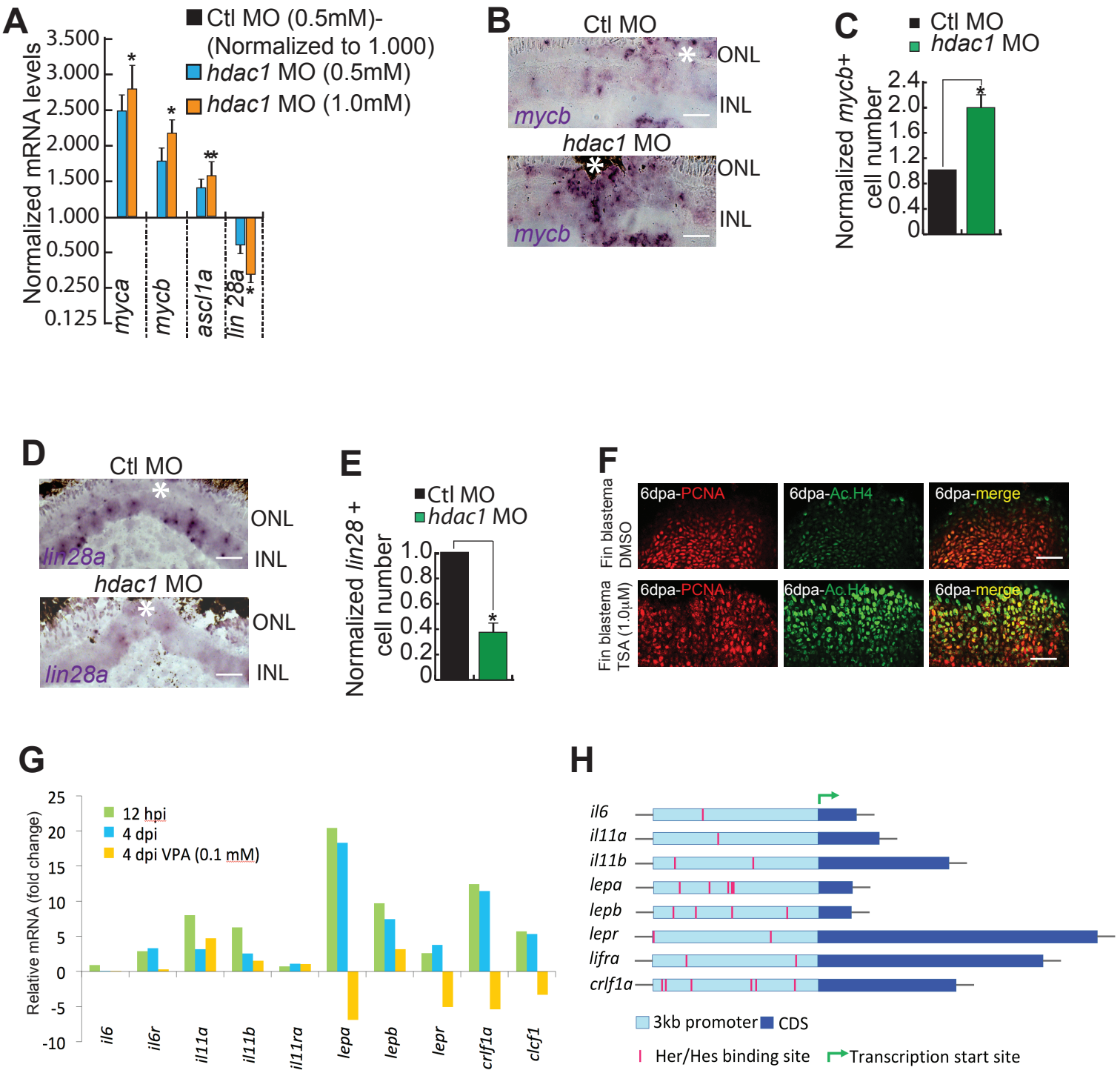
A
Ctl MO (0.5mM)-
(Normalized to 1.000)
hdac1 MO (0.5mM)
hdac1 MO (1.0mM)
Normalized mRNA levels
3.500
3.000
2.500
2.000
1.500
1.000
0.500
0.250
0.125
myca
mycb
ascl1a
lin 28a
B
Ctl MO
ONL
INL
mycb
hdac1 MO
ONL
INL
mycb
C
Ctl MO
hdac1 MO
Normalized mycb+ cell number
2.4
2.0
1.6
1.2
0.8
0.4
0
D
Ctl MO
ONL
INL
lin28a
hdac1 MO
ONL
INL
lin28a
E
Ctl MO
hdac1 MO
Normalized lin28 + cell number
1.0
0.8
0.6
0.4
0.2
0
F
Fin blastema DMSO
Fin blastema TSA (1.0μM)
6dpa-PCNA
6dpa-Ac.H4
6dpa-merge
6dpa-PCNA
6dpa-Ac.H4
6dpa-merge
G
Relative mRNA (fold change)
25
20
15
10
5
0
-5
-10
12 hpi
4 dpi
4 dpi VPA (0.1 mM)
il6
il6r
il11a
il11b
il11ra
lepa
lepb
lepr
crlf1a
clcf1
H
il6
il11a
il11b
lepa
lepb
lepr
lifra
crlf1a
3kb promoter
CDS
Her/Hes binding site
Transcription start site

Figure S6: Effect of Hdac inhibition on regeneration-associated genes, cytokines, in the retina and Ac.H4 levels in fin blastema. Related to Figure 2, Figure 3, Figure 4, Figure 6, and Figure 7.

(**A**) qPCR analysis shows upregulation of *myca*, *mycb*, *ascl1a*, and downregulation of *lin28a*, with MO-mediated *hdac1* repression, in 2dpi retina, $^{*}P<0.01$, $^{**}P<0.02$. (**B-E**) ISH microscopy shows upregulation of *mycb* expression (**B**), causing 100% increase in $mycb^{+}$ cell number (**C**), and decrease in *lin28a* mRNA levels (**D**), which accounts for 60% reduction in $lin28a^{+}$ cell number (**E**), in MO mediated *hdac1* (0.5mM) knockdown in 2dpi retina, $^{*}P<0.03$ in **C**, $^{*}P<0.001$ in **E**. (**F**) Increased acetylated histone (Ac.H4) levels revealed by IF microscopy in fish treated with TSA to block Hdacs, at 6dpa, might account for blocked fin regeneration. (**G**) Representation of the cytokines revealed in RNAseq analysis at 12hpi, 4dpi and 4dpi-VPA treated retina, compared to uninjured control. (**H**) A model representation of the Her4.1/Hes binding sites on the 3kb regulatory sequences of various cytokines. N = 6 biological replicates. Scale bars, 10 μm (**B, D, F**). Error bars are s.d. The asterisk marks the injury site in all.

Table S1

log2 value of fold change from whole reina RNAseq at different time points post injury										
	il6	il6r	il11a	il11b	il11ra	lepa	lepb	lepr	crlf1a	clcf1
12hpi	0.9	2.9	8	6.2656	0.75	20.45	9.69	2.593	12.4237	5.7
4dpi	0.09	3.3	3.164	2.55	1.12	18.3	7.43	3.78	11.44	5.33
4dpi_VPA 100uM	0.00083	0.3135	4.746	1.51792	1.05	-6.85637	3.15146	-5.0201	-5.337	-3.3229

Table S1. List of cytokines regulated in Hdacs inhibited retina. Related to Figure 6 and Figure S6.

The table shows a list of cytokines, mentioned in this study, obtained from RNAseq data that are regulated during various time points, and Hdacs inhibition with VPA, post retinal injury.

Transparent Methods

Animals, retinal injury, fin cut, and drugs.

Zebrafish were grown at 26-28 °C on a 14 h:10 h light/dark cycle in an automated recirculatory system. The *1016 tuba1a:gfp* transgenic fish used in this study have been previously described (Fausett and Goldman, 2006). Embryos used in all assays were obtained by natural breeding. The retinal injury was performed as described previously (Fausett and Goldman, 2006; Veldman et al., 2010). Fish were anesthetized transiently using tricaine methane sulphonate. Later on, the right eye was gently pulled from its socket, and the retina was stabbed 4-8 times (once or twice in each quadrant) through the sclera with a 30-gauge needle inserted up to the length of the bevel. Similarly, after anesthetizing the fish, its fin was amputated with a single vertical cut perpendicular to the fin rays, in relevant experiments, using a sharp sterile scalpel blade. The Notch signaling blocker *N*-[*N*-(3,5-difluorophenylacetyl)-L-alanyl]- *S*-phenylglycine *t*-butyl ester (DAPT), Hdacs blocker Valproic acid (VPA) were made to a stock of 1mM, and Trichostatin A (TSA) was prepared to 100µM in DMSO for various experiments (all drugs were from Sigma-Aldrich). Drugs were delivered, either by dipping the fish into the water containing the drug or by injection to the vitreous of the eye using a Hamilton syringe with a 30-gauge needle. All the experiments were done to a minimum of three times for consistency and s.d.

RNA sequencing and analysis.

RNA was obtained from the total retina of zebrafish from uninjured (control), 12 hours post injury and 4 days post injury, as previously described (Ramachandran et al., 2011) with or without VPA treatment. The RNA sequencing was performed as described previously (Brooks et al., 2012). The data analysis was performed using TopHat and Cufflinks as reported earlier (Trapnell et al., 2012). The Dataset S1 was created using a code developed in Python and the RNAseq data with particular reference to transcription factors, obtained from the database AnimalTFDB2.0 (Zhang et al., 2015), was analyzed using it. The Venn diagrams in Figures S4G and S4H were created using FunRich (Functional Enrichment Analysis Tool; version 3.0) software (Pathan et al., 2015)

Primers and plasmid construction

All the primers are listed in Dataset S2. The promoter of *her4.1* was amplified from zebrafish genomic DNA using primer pairs Xho-*her4.1*pro-F and Bam-*her4.1* pro-R (~4 kb), respectively. The digested PCR amplicons were cloned into a pEL luciferase expression vector to create *her4.1:gfp-luciferase* constructs. The *lin28a:gfp-luciferase*, *insm1a:gfp-luciferase* constructs were described previously (Ramachandran et al., 2010a; Ramachandran et al., 2012). The *lin28a* promoter site-directed mutagenesis was done as described previously(Ramachandran et al., 2010a). GFP was amplified from a pEGFP-c1 plasmid with BamH1-EGFP-F and EcoR1-EGFP-R and cloned into the pCS2^{+} vector. *The hdac1* coding region was amplified from zebrafish cDNA with EcoR1-hdac1-cds-F and Xho1-hdac1-cds-R and then cloned in frame with GFP of pCS2^{+}GFP vector.

Genes like *ascl1a*, *mycb*, *lin28a*, *hdac1*, *hdac3*, *hdac4*, *hdac5*, *hdac6*, *hdac9* and *nicd* were cloned from complementary DNA amplified from zebrafish retinal RNA at 4 dpi using primer pairs Bam-Ascl1a FL-F and Xho-Ascl1a FL-R (~0.6 kb); Bam-*mycb*-F and Xba-*mycb*-R (~1.2 kb); Bam-*lin28a* FL-F and Xho-*lin28a* FL-R (~0.6 kb). Post-

digested PCR amplicons were cloned into their respective enzyme sites in pCS2^{+} plasmid to obtain *CMV:ascl1a*, *CMV:mycb*, and *CMV:lin28a.* All *hdac* genes, *hdac1* (~0.8kb), *hdac3* (~1.1kb), *hdac4* (~1.1kb), *hdac5* (~1kb), *hdac6* (~1kb), and *hdac9* (~1kb) were amplified by PCR and cloned in TOPO TA cloning vector (Invitrogen, catalog number 45-0640). The *nicd* mRNA was prepared by *in vitro* transcription of PCR product, specific to *nicd*, using primer pairs T7-HSP M-F and Sv40-R (~2kb) from a clone of *nicd* driven by Hsp70 promoter. This clone in turn was made in pTAL plasmid vector by digesting an amplicon of *nicd* obtained using PCR primers Hind2X-flag-NICD-F and MluI NICD-R. All primers used in this study are listed in Dataset S2.

For the confirmation of MO activity, an adaptor having respective MO targeted region for *hdac1* and *her4.1* was cloned in pEGFP-N1 at BamHI and HindIII restriction sites, which append in-frame to GFP reporter. The plasmid with and without respective MOs was injected to observe the absence or presence of GFP fluorescence under a fluorescence microscope.

Total RNA isolation, RT-PCR, and qPCR analysis.
Total RNA was isolated from zebrafish retina in all experimental groups using TRIzol (Invitrogen). Combination of oligo-dT and random hexamers was used to reverse-transcribe 5 micro gram of total RNA using Superscript II reverse transcriptase (Invitrogen) to generate cDNA. PCR reactions were done using Taq or Phusion (New England Biolabs) thermo polymerase and gene-specific primers (Dataset S2) with previously described cycling conditions (Ramachandran et al., 2010a). Quantitative PCR (qPCR) was carried out in triplicate with KOD SYBR qPCR mix (Genetix, QKD-201) on a real-time PCR detection system (Eppendorf MasterCycler RealPlex4). The *let-7a* miRNA quantification was done using TaqMan microRNA probes (Applied Biosystems) as per the manufacturer's directives. In brief, the total RNA was reverse transcribed using reverse transcription primer with a stem-loop (Applied Biosystems) and later on, the real-time PCR was performed with a TaqMan PCR kit on an Applied Biosystems Quant Studio 3 detection system. The relative expression of mRNAs in control and injured retinae was deciphered using the ΔΔCt method and normalized to ribosomal protein *l*-24 or *β-actin* mRNA levels.

mRNA synthesis, and embryo microinjection
Various gene clones in pCS2^{+} plasmids having cDNA inserts were linearized, and capped mRNAs were synthesized using the mMESSAGE mMACHINE (Ambion) *in vitro* transcription system. For luciferase assay experiments, single-cell zebrafish embryos were injected with a total volume of ~1nl solution containing 0.02 pg of *Renilla* luciferase mRNA (normalization), 5 pg of *promoter:gfp-luciferase* vector and 0-6 pg of *nicd* mRNA. To further assure the consistency of results, a master mix was made for daily injections, and ~ 300 embryos were injected at the single cell stage. 24 hours later, the embryos were divided into three groups (~ 70 embryos/group) and lysed for dual luciferase reporter assays (Promega, catalog number E1910).

Morpholino electroporation, mRNA transfection, and knockdown-rescue.
Lissamine-tagged MOs (Gene Tools) of approximately 0.5 µl (0.5 to 1.0 mM) was

injected at the time of injury using a Hamilton syringe of 2 µl volume capacity. MO delivery to cells was accomplished by electroporation as previously described (Fausett et al., 2008). The control and *ascl1a* targeting MOs have been previously described (Ramachandran et al., 2012). Morpholinos targeting *hdac1*and *her4.1* are:
hdac1 MO, 5′-TGTTCCTTGAGAACTCAGCGCCATT- 3′ ;
2- *hdac1* MO, 5'-TTACCCTCCAATTACAGCCTGCGCC-3'.
her4.1 MO, 5'-TTGATCCAGTGATTGTAGGAGTCAT-3'

Transfection mixture contained two solutions constituted in equal volumes. (A) 4-5 µg of mRNA mixed with HBSS (Hanks balanced salt solution), (B) Lipofectamine messenger max reagent (Invitrogen, Catalogue number LMRNA001) mixed with HBSS. Both the solutions were allowed to stand at room temperature for 10 minutes and then mixed dropwise followed by 30 minutes incubation at room temperature. The resultant solution was mixed with morpholino in equal proportion, and 0.5 µl of this mixture was used for injection in zebrafish retina followed by electroporation as described earlier.

In vivo rescue experiments were designed for testing the specificity of *hdac1* MO antisense oligos. We did the transfection of zebrafish retina using gene-specific mRNA alongside the MO targeting 5' UTR region of concerned genes or control MO. For confirming the efficient mRNA transfection, GFP mRNA was also delivered by transfection in control retina, whereas GFP fusion with *hdac1* mRNA was used in other sets.

BrdU labeling, Retina tissue preparation for mRNA *in situ* hybridization, immunofluorescence microscopy, TUNEL Assay and Western blotting
BrdU labeling was performed by single intraperitoneal injection of 20 µl of BrdU (20 mM) 3 h before euthanasia and retina dissection unless explicitly mentioned. Some animals required for long-term cell tracing experiments received more BrdU injections over multiple days as described in various timelines mentioned in Figures. Fish were given a higher dose of tricaine methane sulphonate and eyes were dissected, lens removed, fixed in 4% paraformaldehyde and sectioned as described previously (Fausett and Goldman, 2006). RNA *in situ* hybridization (ISH) was performed on retina sections with fluorescein or digoxigenin-labeled complementary RNA probes (FL/DIG RNA labeling kit, Roche Diagnostics) (Barthel and Raymond, 2000). Fluorescence ISH was performed according to the manufacturer's directions (Thermo Fisher Scientific, catalogue numbers T20917, B40955, B40953). Sense probes were used in every ISH separately as control, to assess the potential of the background signal. Immunofluorescence microscopy protocols and antibodies were previously described (Ramachandran et al., 2012). Immunofluorescence microscopy was performed using rabbit polyclonal antibody for acetylated histone 4 of avian origin (Santa Cruz, catalogue number sc-34263); rabbit polyclonal antibody against human ASCL1/MASH1 (Abcam, catalogue number ab74065); Rat monoclonal antibody against BrdU (Abcam, catalogue number ab6326); mouse monoclonal antibody against human proliferating cell nuclear antigen, PCNA (Santa Cruz, catalogue number sc-25280); rabbit polyclonal antibody against zebrafish Myca/b (Schreiber-Agus et al., 1993) (Anaspec, catalogue number AS-55477); Rabbit polyclonal antibody against zebrafish Hdac1 (Harrison et al., 2011) (Abcam, catalogue number ab-41407); mouse polyclonal antibody against GFP (Abcam, catalogue number ab-38689); Rabbit polyclonal antibody against GFP (Abcam,

catalogue number ab-290); Rabbit polyclonal antibody against mouse glutamine synthetase (Ramachandran et al., 2010b) (Abcam, catalogue number ab93439) at 1:500 dilution. Before BrdU immunofluorescence microscopy, retinal sections were treated with 2 N HCl at 37 °C for 20 min, equilibrated with 100mM sodium borate (pH 8.5) for 10 min, twice and then processed using standard procedures (Senut et al., 2004). BrdU labeled MGPC lineage-tracing experiments were done in retinal sections from eye sections of 8 microns thickness, distributed across five slides. An individual slide was first processed for immunofluorescence-based detection of specific antigen or mRNA, and then BrdU or PCNA staining was performed as mentioned above using respective antibodies (Powell et al., 2012; Ramachandran et al., 2012). The total number of $BrdU^+$ cells and the number of co-labeled $BrdU^+$ cells that also stained with a specific ISH probe and subsequent enzymatic reaction were quantified on each slide. TUNEL assay was performed on retinal sections using In Situ Cell death Detection Fluorescein kit (Roche, Ref no:11684795910) as per manufacturer recommended protocol. Western blotting was performed using whole retina tissue using 4 retinae per experimental sample, lysed in Laemmli buffer, size fractioned in 12% acrylamide gel with SDS at denaturing conditions before transferring on to Immun-Blot PVDF membrane (Biorad Catalogue number 162-0177), followed by probing with specific primary antibodies and HRP conjugated secondary for chemiluminescence assay using Clarity Western ECL (Biorad Catalogue number 170-5061).

Fluorescence and confocal microscopy, cell counting, statistical analysis and software.

Every section of the stained retina was mounted, visualized and analyzed, and at least three retinae from separate fish were used. After the staining experiments, the slides were examined with a Nikon N*i*-E fluorescence microscope equipped with fluorescence optics and Nikon A1 confocal imaging system. Cell counts were quantified by physically observing fluorescently labeled ISH, PCNA or $BrdU^+$ cells in retinal sections, visualized in the same microscope. Observed data were analyzed for statistical significance by comparisons done using a two-tailed unpaired Student's *t*-test to analyze data from all experiments. For all other comparisons, analysis of variance (ANOVA) was performed followed by *post hoc t*-test using Stat View software. Transcription factor binding sites are predicted using TRANSFAC platform (http://genexplain.com/transfac/), which are later verified manually.

Fluorescence-based cell sorting.

RNA was obtained from FACS purified MG and MG-derived progenitors at 4 dpi as previously described (Ramachandran et al., 2011, 2012). The uninjured and injured retinae were isolated from *1016 tuba1a:gfp* transgenic fish. GFP+ MGPCs from *1016 tuba1a:gfp* retinae at 4 dpi were isolated by treating retinae with hyaluronidase and trypsin and then sorted on a BD FACS Aria Fusion high-speed cell sorter. Approximately 30 injured retinas from *1016 tuba1a:gfp* fish yielded 70,000 GFP+ and 150,000 GFP- cells.

References

Barthel, L.K., and Raymond, P.A. (2000). In situ hybridization studies of retinal neurons. Methods Enzymol *316*, 579-590.

Brooks, M.J., Rajasimha, H.K., and Swaroop, A. (2012). Retinal transcriptome profiling by directional next-generation sequencing using 100 ng of total RNA. Methods Mol Biol *884*, 319-334.

Fausett, B.V., and Goldman, D. (2006). A role for alpha1 tubulin-expressing Muller glia in regeneration of the injured zebrafish retina. J Neurosci *26*, 6303-6313.

Fausett, B.V., Gumerson, J.D., and Goldman, D. (2008). The proneural basic helix-loop-helix gene ascl1a is required for retina regeneration. J Neurosci *28*, 1109-1117.

Harrison, M.R., Georgiou, A.S., Spaink, H.P., and Cunliffe, V.T. (2011). The epigenetic regulator Histone Deacetylase 1 promotes transcription of a core neurogenic programme in zebrafish embryos. BMC Genomics *12*, 24.

Pathan, M., Keerthikumar, S., Ang, C.S., Gangoda, L., Quek, C.Y., Williamson, N.A., Mouradov, D., Sieber, O.M., Simpson, R.J., Salim, A.*, et al.* (2015). FunRich: An open access standalone functional enrichment and interaction network analysis tool. Proteomics *15*, 2597-2601.

Powell, C., Elsaeidi, F., and Goldman, D. (2012). Injury-dependent Muller glia and ganglion cell reprogramming during tissue regeneration requires Apobec2a and Apobec2b. J Neurosci *32*, 1096-1109.

Ramachandran, R., Fausett, B.V., and Goldman, D. (2010a). Ascl1a regulates Muller glia dedifferentiation and retinal regeneration through a Lin-28-dependent, let-7 microRNA signalling pathway. Nat Cell Biol *12*, 1101-1107.

Ramachandran, R., Reifler, A., Parent, J.M., and Goldman, D. (2010b). Conditional gene expression and lineage tracing of tuba1a expressing cells during zebrafish development and retina regeneration. J Comp Neurol *518*, 4196-4212.

Ramachandran, R., Zhao, X.F., and Goldman, D. (2011). Ascl1a/Dkk/beta-catenin signaling pathway is necessary and glycogen synthase kinase-3beta inhibition is sufficient for zebrafish retina regeneration. Proc Natl Acad Sci U S A *108*, 15858-15863.

Ramachandran, R., Zhao, X.F., and Goldman, D. (2012). Insm1a-mediated gene repression is essential for the formation and differentiation of Muller glia-derived progenitors in the injured retina. Nat Cell Biol *14*, 1013-1023.

Schreiber-Agus, N., Horner, J., Torres, R., Chiu, F.C., and DePinho, R.A. (1993). Zebra fish myc family and max genes: differential expression and oncogenic activity throughout vertebrate evolution. Mol Cell Biol *13*, 2765-2775.

Senut, M.C., Gulati-Leekha, A., and Goldman, D. (2004). An element in the alpha1-tubulin promoter is necessary for retinal expression during optic nerve regeneration but not after eye injury in the adult zebrafish. J Neurosci *24*, 7663-7673.

Trapnell, C., Roberts, A., Goff, L., Pertea, G., Kim, D., Kelley, D.R., Pimentel, H., Salzberg, S.L., Rinn, J.L., and Pachter, L. (2012). Differential gene and transcript expression analysis of RNA-seq experiments with TopHat and Cufflinks. Nat Protoc *7*, 562-578.
Veldman, M.B., Bemben, M.A., and Goldman, D. (2010). Tuba1a gene expression is regulated by KLF6/7 and is necessary for CNS development and regeneration in zebrafish. Mol Cell Neurosci *43*, 370-383.
Zhang, H.M., Liu, T., Liu, C.J., Song, S., Zhang, X., Liu, W., Jia, H., Xue, Y., and Guo, A.Y. (2015). AnimalTFDB 2.0: a resource for expression, prediction and functional study of animal transcription factors. Nucleic Acids Res *43*, D76-81.